# sCO2-4-NPP: Innovative sCO2-Based Heat Removal Technology for an Increased Level of Safety of Nuclear Power Plants

# Deliverable 4.6

# Final conceptual design of the Heat Recovery Exchanger

*Work programme topic addressed: NFRP-2018-10: Encouraging innovation in nuclear safety for the benefit of European citizen*

*Type of action: Innovation action*

| | |
|---|---|
| Grant Agreement number: | 847606 |
| Start date of project: 1 September 2019 | Duration: 36 months |
| Lead beneficiary of this deliverable: | CVR |
| Due date of deliverable: 31/08/2022 | Actual submission date: 31/08/2022 |
| | Version #: R1.0 |

| Type | | |
|---|---|---|
| R | Document, report excluding the periodic and final reports | X |
| DEM | Demonstrator, pilot, prototype, plan designs | |
| DEC | Websites, patents filing, press & media actions, videos, etc. | |
| OTHER | Software, technical diagram, etc. | |
| **Dissemination level** | | |
| PU | PUBLIC, fully open, e.g. web | X |
| CO | CONFIDENTIAL, restricted under conditions set out in Model Grant Agreement | |

This project has received funding from the Euratom research and training programme 2014-2018 under grant agreement No 847606. This document and its contents remain the property of the beneficiaries of the sCO2-4-NPP Consortium and may not be distributed or reproduced without the express written approval of the Coordinator, EDF.

# Revision History

| Release | Date | Reason for Change | Author | Distribution |
|---|---|---|---|---|
| R0.1 | 12/08/2022 | First draft | R. Filip | All partners |
| R0.2 | 15/08/2022 | Submission for review | R. Filip | All partners |
| R1.0 | 31/08/2022 | Final version | R. Filip | Public |

# Deliverable Contributors

### *Authors*

| Partner | Name |
|---|---|
| CVR | Radomir Filip |

### *Contributors*

| Partner | Name |
|---|---|
| FIVES | Sarah Tioual-Demange |
| CVR | Otakar Frýbort |
| CVR | Petr Hájek |

### *Internal Reviewers*

| Partner | Name |
|---|---|
| USTUTT | Jörg Starflinger |
| EDF | Albannie Cagnac |

# Table of contents

# List of Tables

# List of Figures

# 1 Nomenclature and List of Acronyms

| Nomenclature | Description/meaning |
|---|---|
| $A$ | Total heat transfer area; m$^2$ |
| $Af$ | Fins heat transfer area; m$^2$ |
| $DH$ | Hydraulic diameter; m |
| $f$ | Fanning friction coefficient; (-) |
| $G$ | Mass-flow per flow cross-section; kg/(s.m$^2$) |
| $H$ | Channel height; m |
| $k$ | Thermal conductivity; W/(m.K) |
| $L$ | Effective length; m |
| $\dot{m}$ | Mass flow; kg/s |
| $N$ | Number of channels; (-) |
| $Nu$ | Nusselt number; |
| $p$ | pressure; Pa |
| $P$ | Channel Pitch; m |
| $Pr$ | Prandtl number; |
| $\dot{Q}$ | Transferred heat; W |
| $R$ | Thermal resistance; W/(m$^2$.K) |
| $Re$ | Reynolds number; |
| $t$ | Fin thickness; m |
| $T$ | Temperature; °C |
| $U$ | Over all heat transfer coefficient; W/(m$^2$.K) |
| $w$ | flow velocity; m/s |
| $W$ | gas mass fraction |
| $y$ | gas mole fraction |
| **Greek letters** | |
| $\Delta$ | difference |
| $\rho$ | Density; kg/m$^3$ |
| $\mu$ | Dynamic viscosity; Pa.s |
| $\eta 0$ | Total surface effectiveness; (-) |
| $\eta f$ | Fin efficiency; (-) |

| **Acronyms and abbreviations** | |
|---|---|
| *CAPEX* | Capital expenditure |
| *FPM* | fins per meter |
| *htc* | heat transfer coefficient, W/($m^2$.K) |
| *LMTD* | Logarithmic mean temperature difference; °C |
| *VVER* | water-water energy reactor |
| **Subscripts** | |
| *g* | gas |
| *l* | liquid |
| *s* | solid |
| *sat* | saturated |

# 2 Executive Summary

This deliverable deals with studies of the heat recovery exchanger of the project sCO2-4-NPP, specifically the compact heat exchanger (CHX). This component forms an interface between the water/steam circuit of a nuclear power plant and the dedicated $sCO_2$ loop for potential decay heat removal during accidental scenarios. Extensive experimental work was performed to study thermal-hydraulic performance of such a heat exchanger at relevant parameters (up to 285 °C / 7 MPa on the water side, up to 14 MPa / 270 °C on the $sCO_2$ side). For this purpose, a unique experimental stand allowing natural convection water/steam flow equipped with a 27 kW boiler and CHX mock-up and coupled with the existing $sCO_2$ loop was designed, built and commissioned at CVR. The CHX mock-up was fabricated and delivered to CVR by FIVES. In this report, the experimental layout and results are presented and evaluated including an assessment of heat transfer and pressure drop performance. Moreover, a design study of a large-scale (10 MW) CHX including CAPEX estimate is also presented.

# 3 Introduction

This document was made within the sCO2-4-NPP project [1], which aims to utilize the $sCO_2$ cycle as an additional safety system, serving mainly in case of the station blackout (SBO) to remove the decay heat from the nuclear power plants. Such a system primarily consists of a compact heat exchanger, turbomachinery with coupled compressor and turbine and air cooled heatsink (schematically shown in Figure 1).

The subject of this document is mainly focused on the heat transfer between the steam and $sCO_2$, which is mediated by the Compact Heat Exchanger (CHX). The CHX forms an interface between the secondary circuit of PWR (or the primary circuit of BWR) and the dedicated $sCO_2$ loop. This component should be able initiate the self-propelling circulation on the steam side and have rather small size that the retrofitting into an existing powerplant is possible.

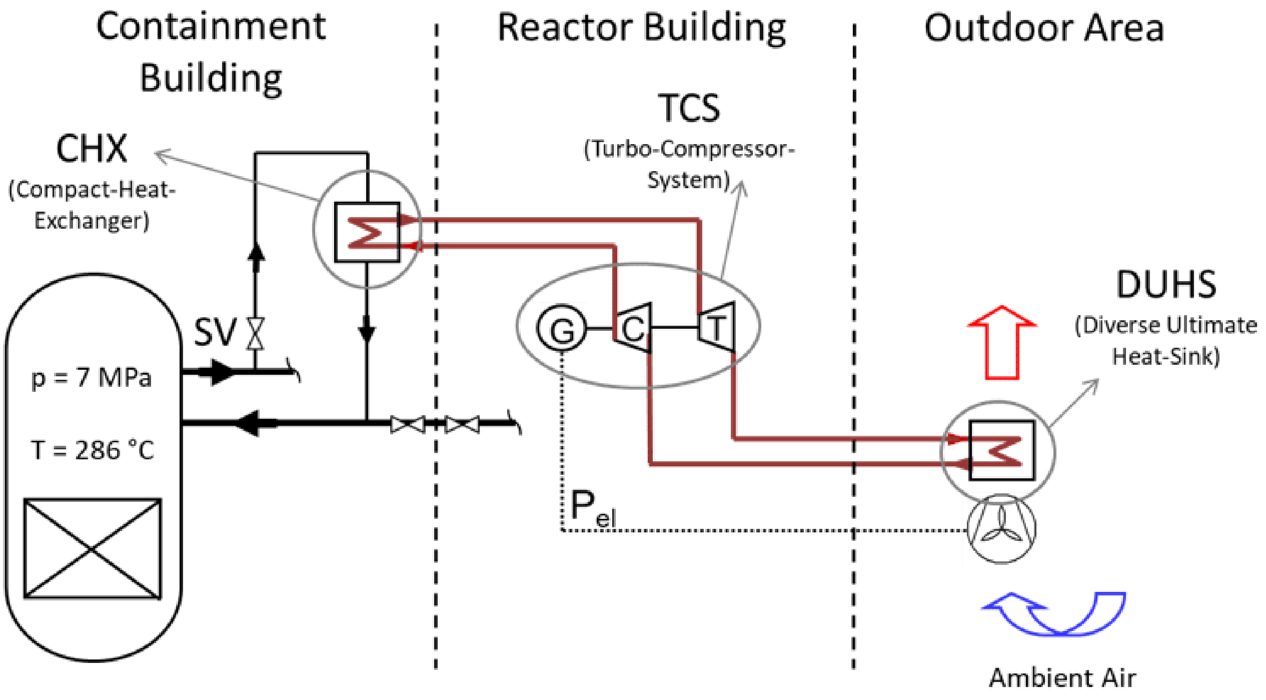

**Figure 1: $sCO_2$ heat removal system attached to a BWR** [2].

The heat transfer phenomena in the compact heat exchanger with $sCO_2$ and steam were previously studied by [2],[3],[4], where the thermal-hydraulic performance of a small scale (<1 kW) compact plate heat exchanger was experimentally tested and numerically validated.

During the sCO2-4-NPP project activities in work package 4, a new CHX preliminary design was developed by FIVES [6]. This new design is based on brazed plates and fin heat exchanger technology and it should be capable of transferring 10 MW of heat. Alongside a small-scale mockup version was fabricated, based on the same channel geometry, in order to test and verify its thermal-hydraulic performance with wider operational parameters. For this purpose, an experimental stand composed of a 27 kW steam generator, pipelines, CHX mock-up and other necessary equipment was built and coupled with the exiting $sCO_2$ loop of CVR that ensures testing at the relevant parameters.

The biggest limiting factor with naturally driven condensation is the presence of non-condensable gases, which significantly affect the heat transfer and often is neglected in thermodynamical analyses. According to [7] in case of free convection (free stream velocity is zero) in the air-steam mixture with air concertation only 0.1 %, the heat transfer decreases by about 32 %. The heat transfer decreases further with higher air concentrations in the air-steam mixture. The reason for this is briefly that the non-condensable gases present in the steam mixture start to concentrate along the core of the condensation channel, causing the concentration gradient between the liquid water. Since the liquid water is undercooled, the non-condensable gases tend to diffuse back and creating barrier for the water steam to condense.

Another study [8] shows the same effect during the forced convection ($Re_g = 4{\cdot}10^4$) in a vertical tube, where the presence of the non-condensable gas with a concentration of 1 % decreases the heat transfer along the surface by about 20 % as it is shown in Figure 2. In this case, the vapor shear created by the free stream velocity causes a thinning of the condensate film near the top of the vertical tube and thus enhancing the heat transfer. Furthermore, it sweeps the gases from the heat transfer surface, hence reducing the local effect of the non-condensable gases on heat transfer.

The water in the secondary reactor cooling system, where the CHX is intended to connect, contains some amount of non-condensable gases, which are normally dissolved and can be released either by a decrease of pressure or by a change of temperature leading to lower gas solubility. The primal source of the non-condensable gases comes from the additives preventing corrosion, added in the cooling water. The cooling water chemistry is strictly monitored, where for example the oxygen concentration limit in a VVER power reactor is 0.005 $mg/dm^3$ [9], however there is no limit for nitrogen, which content can be about 15 Nml/kg [10]. To ensure the proper function of the steam power cycle during the normal operation, the non-condensable gases must be continuously vented from the condenser with vacuum pumps.

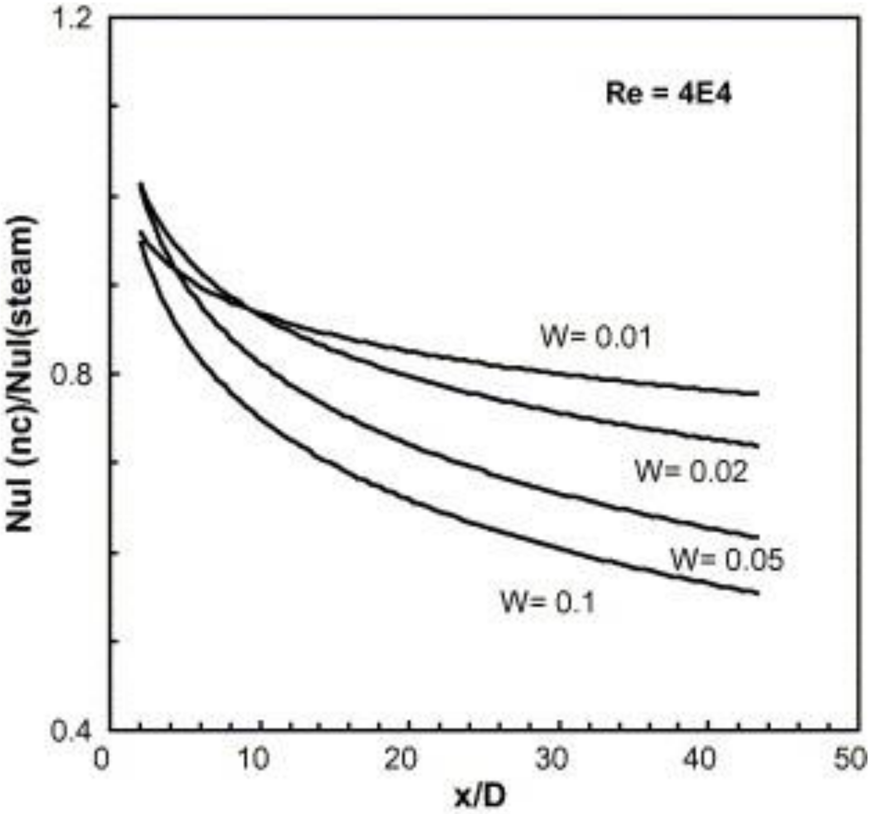

**Figure 2: The axial profile of the average heat transfer coefficient for 16 mm diameter pipe for different non-condensable gas concentration at inlet Re = 4·10$^4$** [8]**.**

# 4 Data collection for steam condensation in tiny channels

## 4.1 CHX mock up design

To test the thermal-hydraulic performance of the CHX preliminary design a small mockup version was fabricated. The channel geometry of the mockup heat exchanger is based on the preliminary design version and it is present in Table 1. The mockup is 430 mm in length, 160 mm in width and height is 42 mm. It contains 4 passages for the steam and 3 passages for the $sCO_2$ [11]. There is a 1 mm thick separator plate between each passage. The whole CHX mockup was fabricated from stainless steel 316L, it is shown in Figure 3.

**Table 1: CHX mock up fin geometry.**

| | $CO_2$ side fins | | Steam side fins | |
|---|---|---|---|---|
| | Distributors | Exchange | Distributors | Exchange |
| **Thickness t (mm)** | 0.3 | | | |
| **Type** | Plain | | | |
| **Height h (mm)** | 4 | | | |
| **FPM p (Fins Per meter)** | 787.4 | | 393.7 | |
| **Fins geometry sketch** | 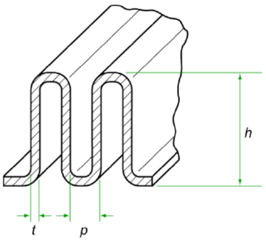 | | 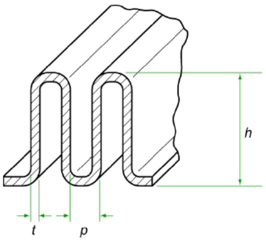 | |

**Figure 3: CHX mock up.**

## 4.2 Testing facility and experimental layout

The heat exchanger testing took place at Research Centre Rez (CVR) using $sCO_2$ experimental loop, which was constructed within SUSEN (Sustainable Energy) project [12]. The $sCO_2$ loop is a large-scale experimental facility in the form of a simple Brayton cycle with the heating power 110 kW, $sCO_2$ temperatures up to 550 °C, pressure 25 MPa and mass-flow rate up to 0.3 kg/s. The facility has been used within various R&D projects focused on the development of $sCO_2$ cycles and the components testing. The CHX mock-up was delivered by FIVES to CVR and was implemented in the high-pressure part of the $sCO_2$ loop which corresponds to appropriate location in the real $sCO_2$ cycles, shown in Figure 4.

For the steam side of the heat exchanger, an additional closed steam loop was fabricated, which can deliver saturated steam at pressures up to 8 MPa (295 °C). The scheme of the steam loop is shown in Figure 5, where the main part consists of the steam boiler with volume of 63 l, which is equipped with electrical heating rods of the nominal power of 27 kW. The hot leg leading into the CHX mockup is equipped with additional heating cords to ensure the steam enters slightly superheated. The hot inlet on the steam side is approximately 2.6 m above the water level in the boiler. The cold leg of the CHX mockup is connected back to the boiler under the water level, closing the loop. There is an additional gas outlet connected to the cold leg of the CHX mockup, allowing manual release of the accumulated non condensable gases. The water reservoir with a volume of 90 l is decoupled from the high pressure during the operation and serves as a water storage, prior the operation, when the high pressure side is vacuumed. Demineralized water was used for the experiments, which was kept under a pure nitrogen atmosphere at constant 1.1 $bar_{(a)}$ pressure. The installed instrumentation with its measurement error is listed in Table 2 and its position is illustrated in Figure 5. The overall view of the experimental setup is shown in Figure 6.

The experimental stand was designed, fabricated and commissioned exclusively within the sCO2-4-NPP project at CVR according to the relevant standards and quality requirements.

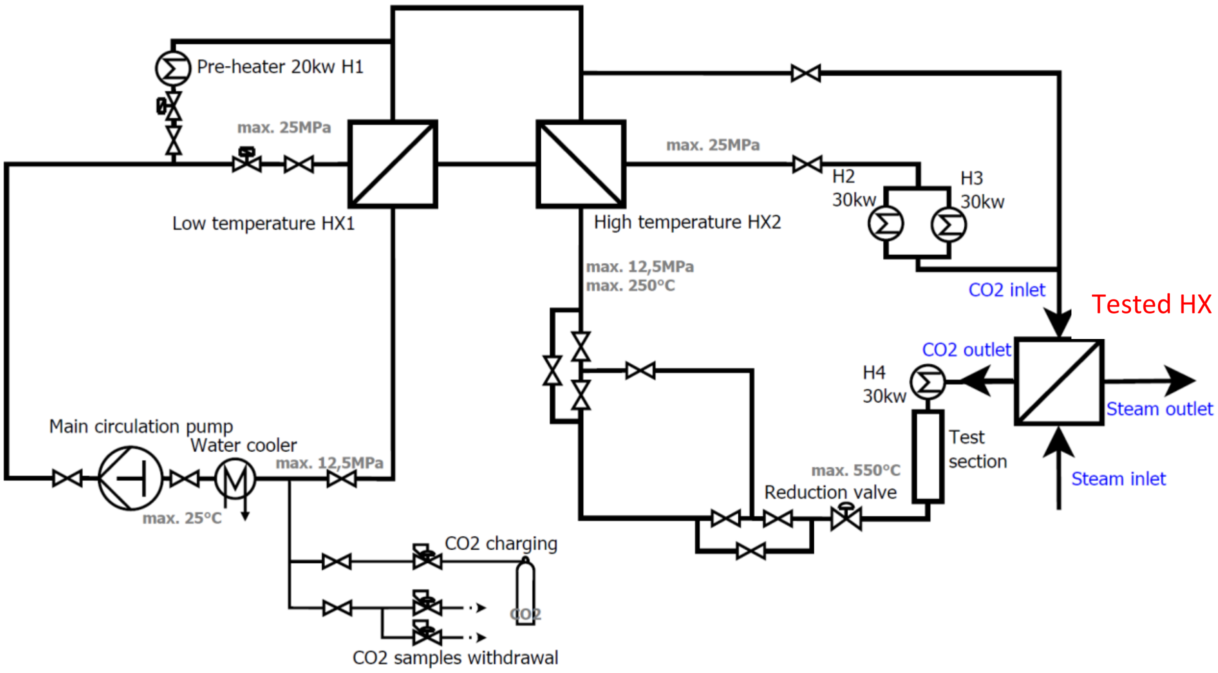

Figure 4: Scheme of the experimental $sCO_2$ loop.

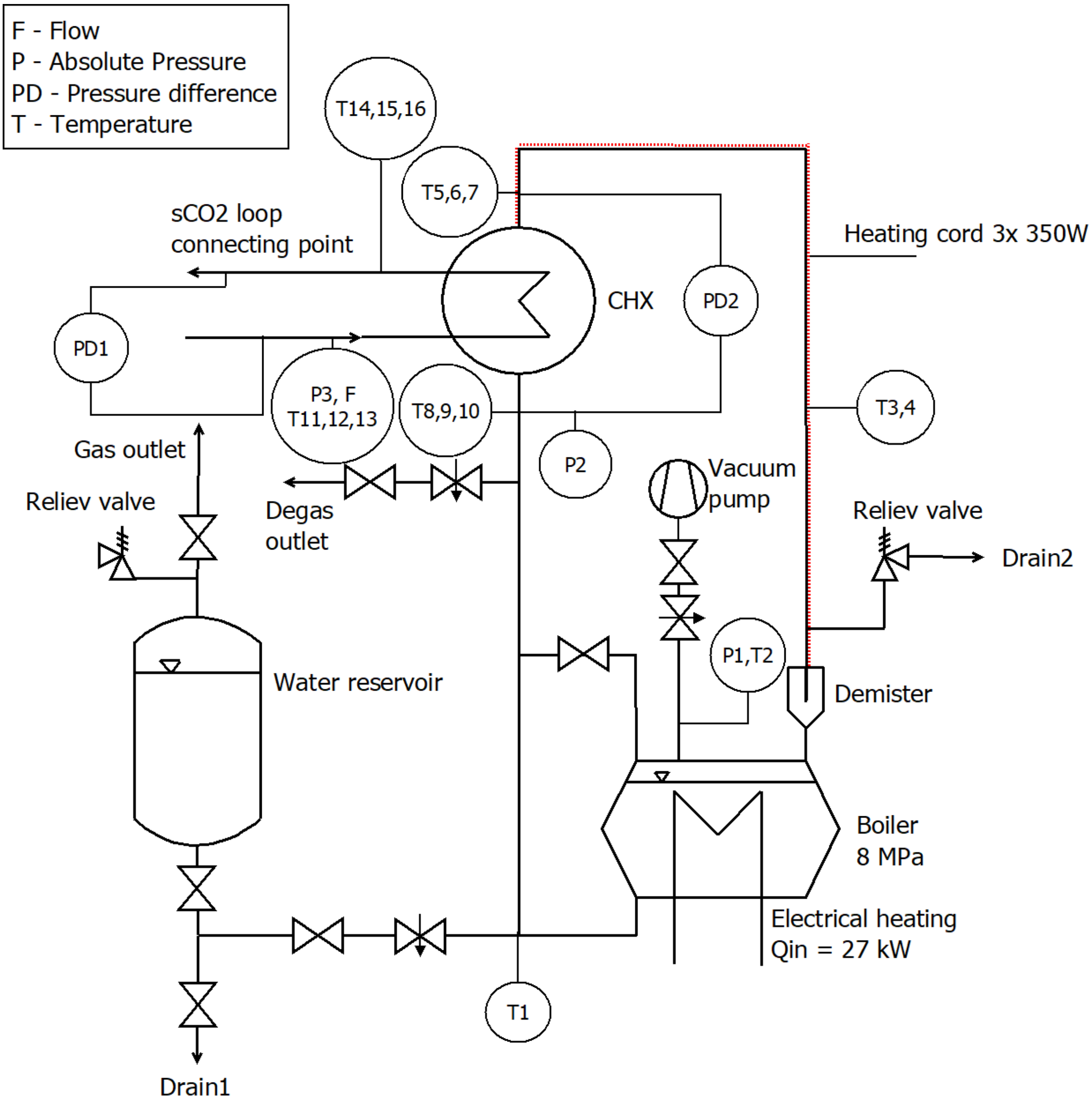

Figure 5: Experimental layout of the steam side.

Table 2: List of used instrumentation.

| Variable | Description | Range | Units | Measurement error |
|---|---|---|---|---|
| **T1-4** | K-type thermocouple class 1 | 0-300 | °C | ± 1.5 °C |
| **T5-16** | Pt100 class A | 0-300 | °C | ± 0.35 °C |
| **F** | Coriolis flow meter | 0-0.7 | kg/s | ± 10% of measured value |
| **PD1** | Pressure difference transducer | 0-5000 | mbar | ± 4 mbar |
| **PD2** | Pressure difference transducer | 0-500 | mbar | ±0.4 mbar |
| **P1-3** | Absolute pressure transducer | 0-400 | bar | ±0.3 bar |

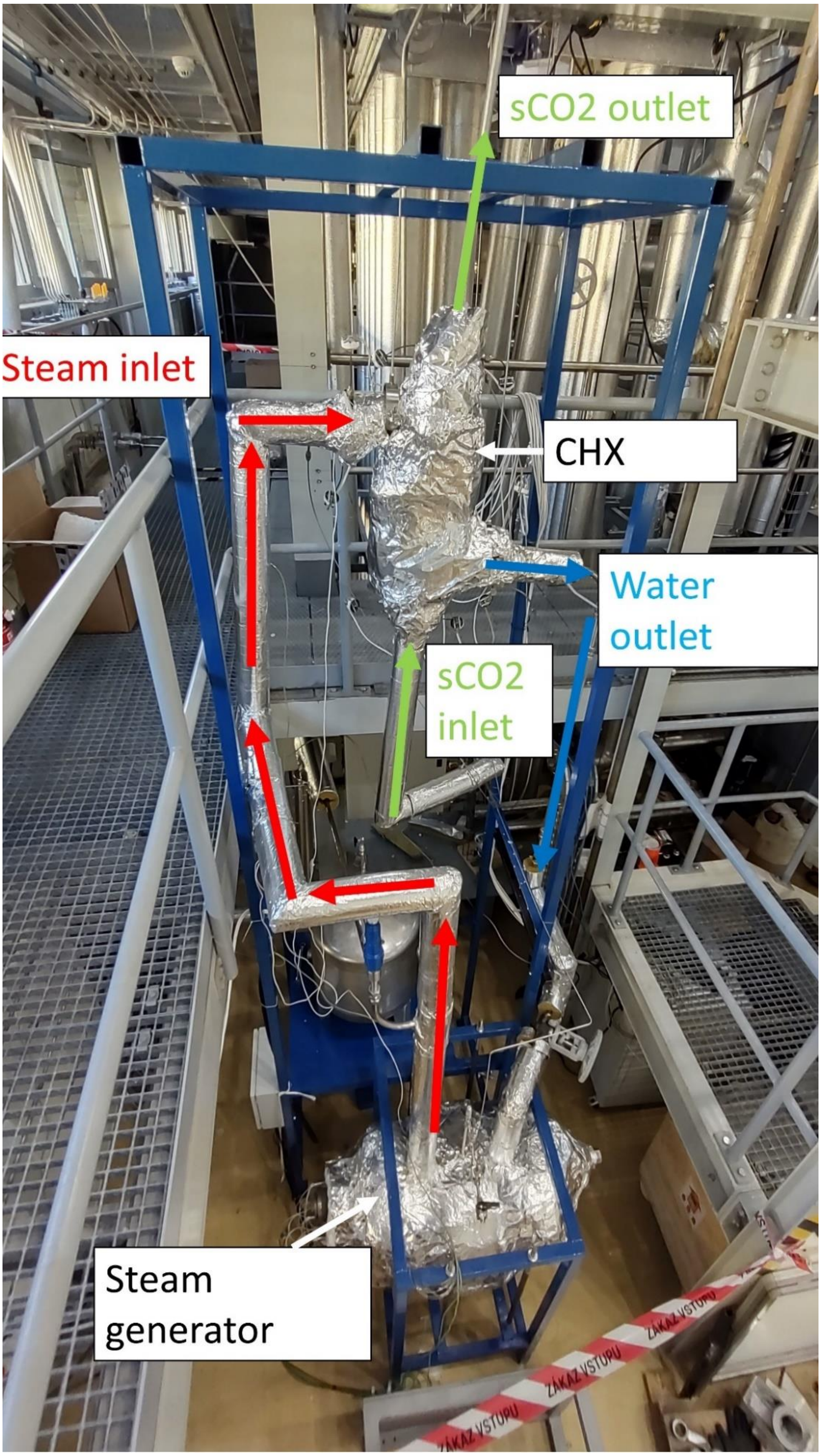

**Figure 6: Experimental setup with connected CHX.**

## 4.3 Experimental results

During the experimental campaign, which lasted for 50 h, 20 steady state cases were measured. Each of the inlet/outlet of the CHX mockup was equipped with 3 Pt100 thermistor, where the final temperature was considered as an average of the 3 values. The measured temperatures for each case are presented in Figure 7 followed by measured absolute pressures, shown in Figure 8. The temperatures and pressures on the $sCO_2$ were kept high enough from the critical point to ensure the super critical state. The measured inlet temperatures on the steam side correspond with measured pressures at saturated states. On the steam outlet a little undercooling with difference in average of 4.4 °C was measured over all cases. This undercooling would correspond to significantly lower absolute pressures, considering there is only water/steam mixture. However, the measured absolute pressure *P2* at the steam outlet more or less matches the pressure *P1*, hence this difference is considered to be the partial pressure of the non-condensable gases. Assuming the non-condensable gases consist of pure nitrogen, its amount can be estimated as a mass fraction according to:

$$W_g = y_{N_2} \frac{\rho_{N_2}}{\rho_{mixture}} \tag{4-1}$$

Where the $y_{N_2}$ can be expressed as:

$$y_{N_2} = \frac{\left(P_2 - P_{sat(Tout,x=0)}\right)}{P_2} \tag{4-2}$$

Despite the efforts to get rid of the majority of non-condensable gases by boiling them off and venting them out prior to the experiments at temperature of 120 °C and yet still significant amount remained. The mass fraction of non-condensable gases is plotted as a function of the absolute pressure shown in Figure 9, where a certain trend can be observed that with increased pressure, the fixed amount of non-condensable gases decreases.

The $sCO_2$ mass flow is plotted in Figure 10, where the mass flow was kept in interval <90; 180> g/s. The transferred heat was then calculated from the enthalpy balance and it is plotted in Figure 11, where the maximum transferred heat reached almost a value of 18 kW. This point corresponds to a highest temperature gradient between the steam inlet and $sCO_2$ inlet, which was 110 °C. The steam/water mass flow was calculated from enthalpy balance and it is plotted in Figure 12. The measured pressure drops on the steam side and the $sCO_2$ side are shown in Figure 13 and Figure 14 respectively.

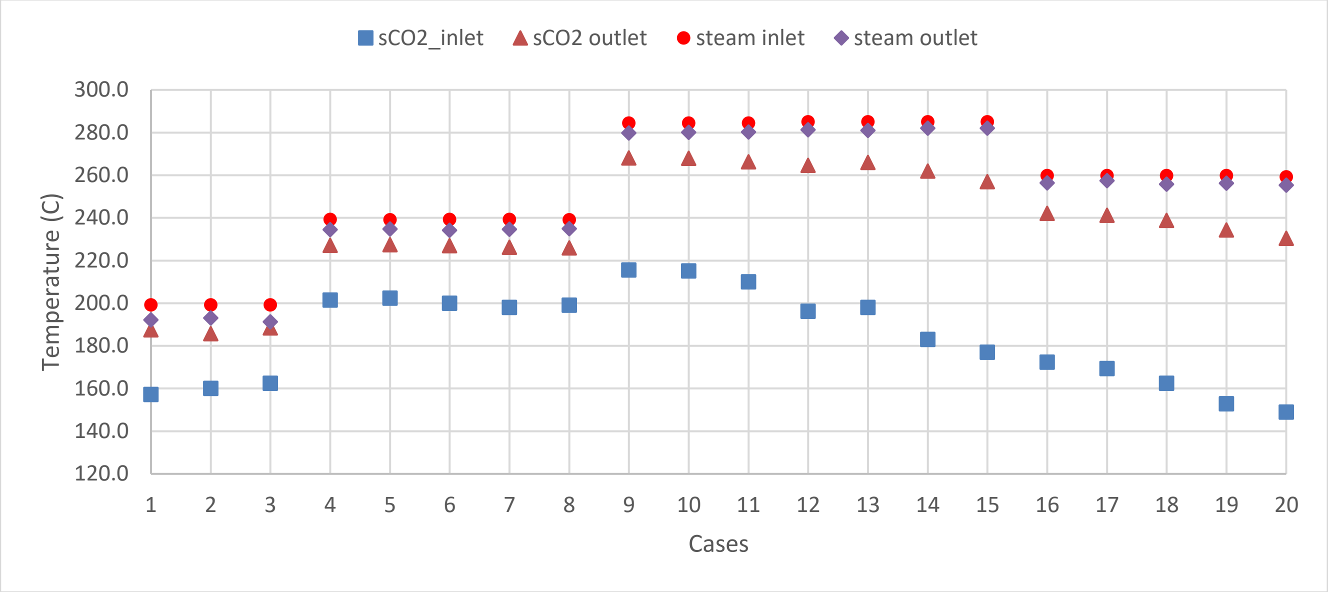

**Figure 7: CHX mockup - experimental data. Temperatures.**

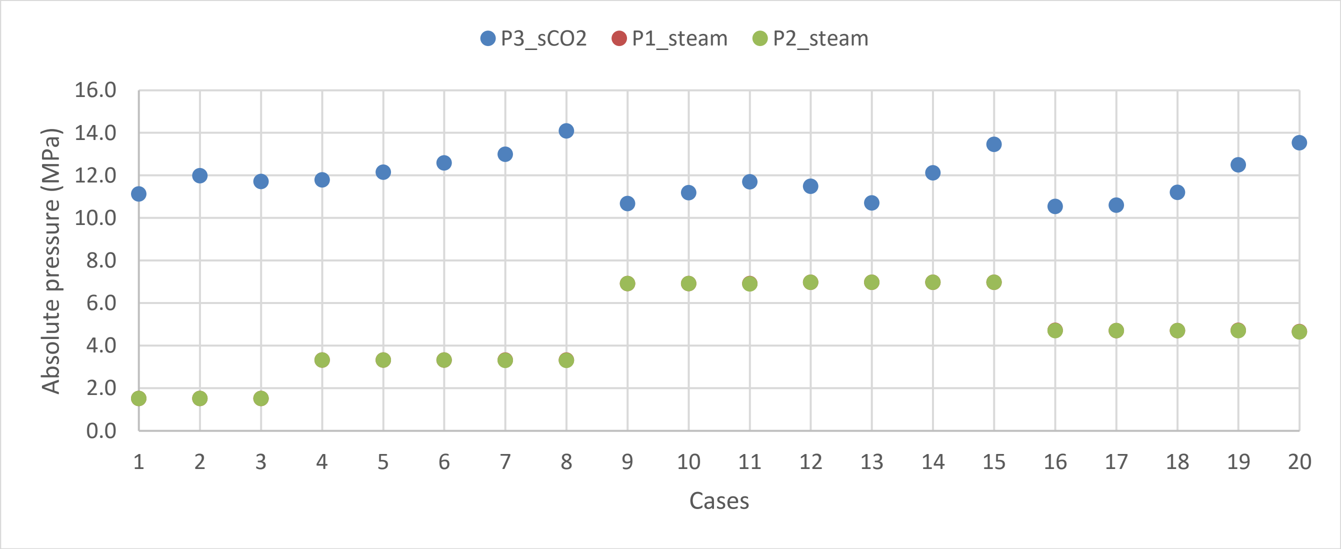

**Figure 8: CHX mockup - experimental data. Absolute pressures.**

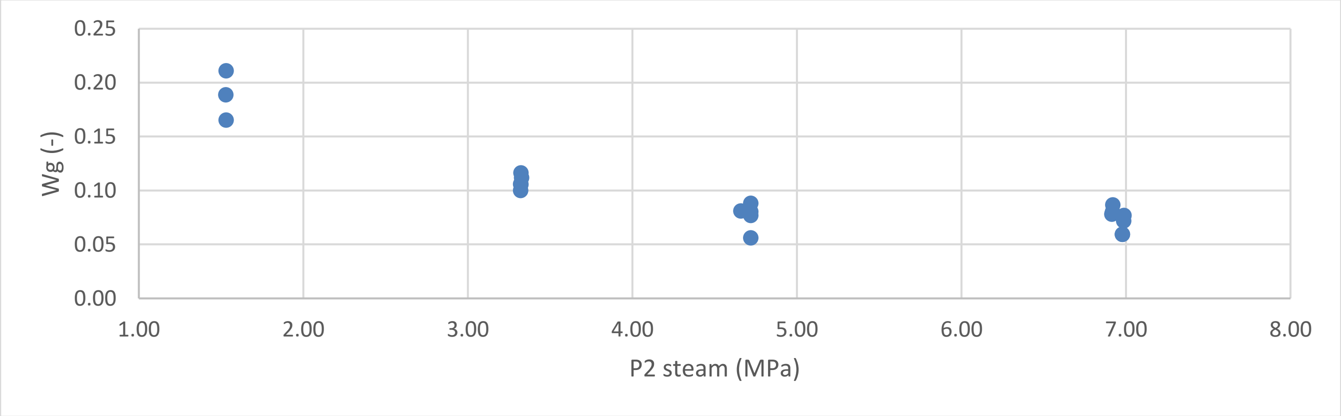

**Figure 9: Estimated amount of non-condensable gases.**

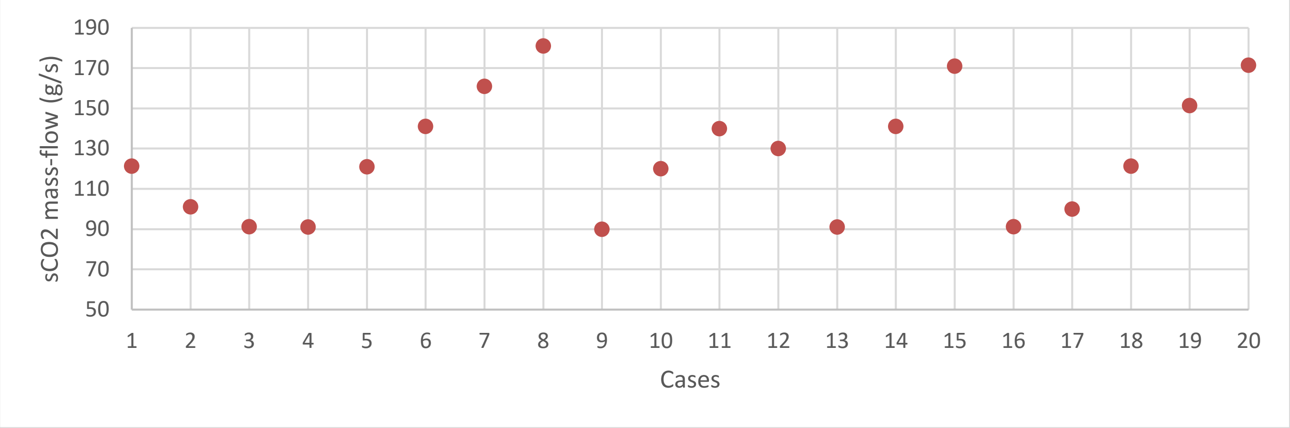

Figure 10: CHX mockup - experimental data. $sCO_2$ mass-flow.

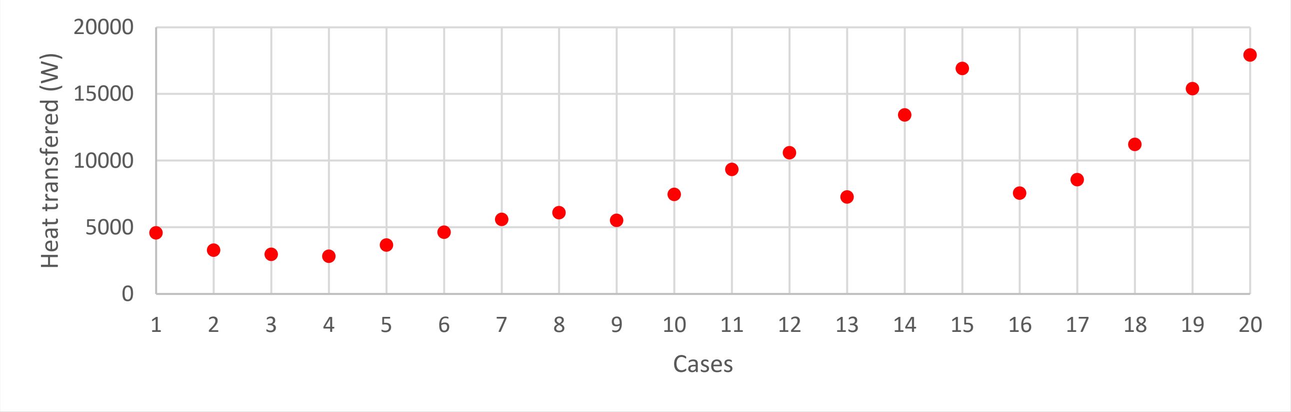

Figure 11: CHX mockup - experimental data. Heat transferred.

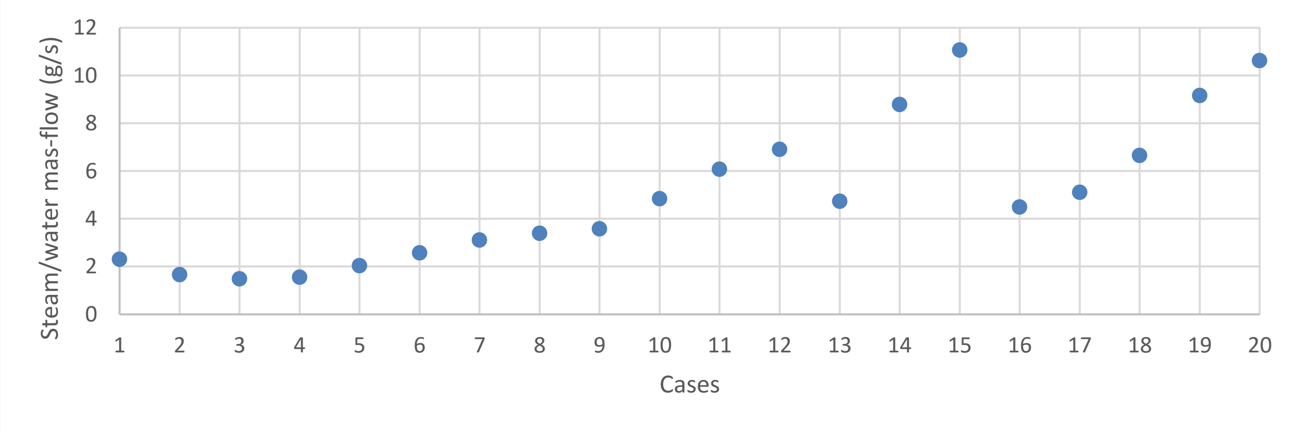

Figure 12: CHX mockup - experimental data. Steam/water mass-flow.

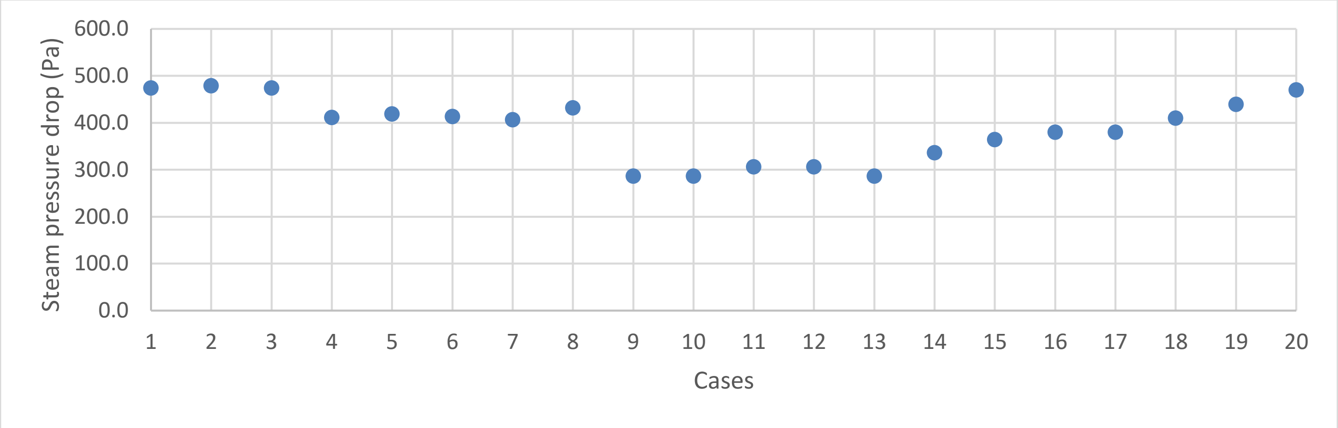

**Figure 13: CHX mockup - experimental data. Pressure drop on the steam side.**

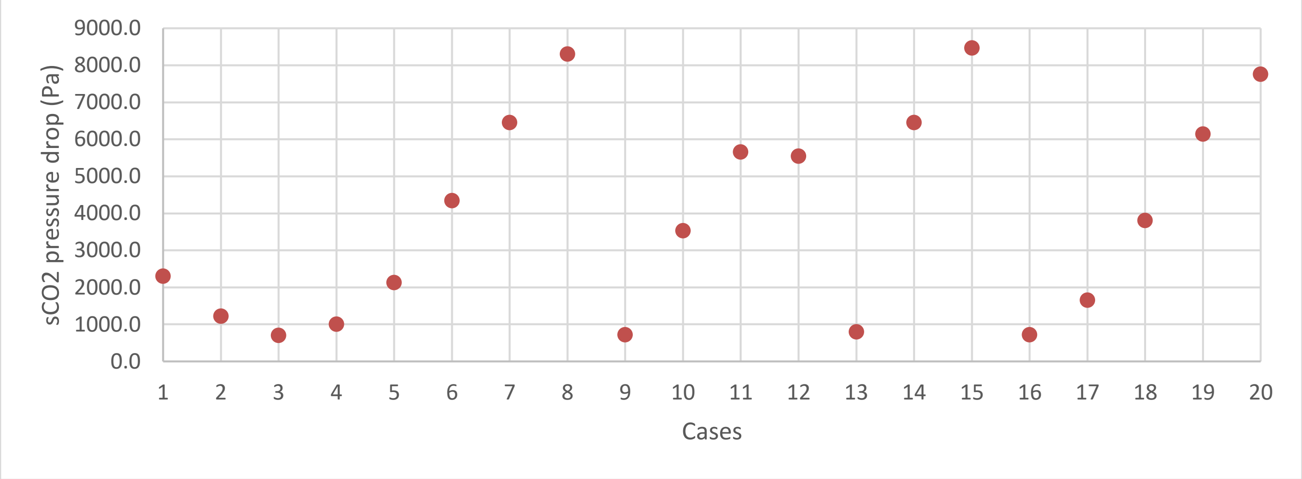

**Figure 14: CHX mockup - experimental data. Pressure drop on the sCO$_2$ side.**

### 4.3.1 Friction fanning factor on the steam side

The fanning friction factor can be determined from the experimental data with following equation [7]:

$$f = \frac{2\, \Delta P\, D_h}{L\, \rho_g w_g^2} \qquad (4\text{-}3)$$

The pressure losses during the natural convection condensation are also affected by flow conditions of the cooling medium as it can be seen in [13]. In order to predict the fanning friction factor with sufficient accuracy, following correlation based on dimensionless number was proposed:

$$f = C \frac{1}{Re_g^m} \left( \frac{\dot{Q}}{\dot{m}\, w_g^2} \right)^n \qquad (4\text{-}4)$$

Where *C, m, n* are constants, $\dot{m}$ is the mass flow, $\dot{Q}$ is the transferred heat, $w_g$ is the vapor velocity and $Re_g$ is the vapor Reynolds number defined as:

$$Re_g = \frac{G\,D_h}{\mu_g} \qquad (4\text{-}5)$$

The fanning friction factor was calculated according to equation ( 4-3 ) and correlated using the least square linear regression method with proposed dimensionless numbers. The resulting correlation for the fanning friction factor on the steam side during the natural convection goes as:

$$f = 254\,\frac{1}{Re_g^{1.41}}\left(\frac{\dot{Q}}{\dot{m}\,w_g^2}\right)^{0.33} \qquad (4\text{-}6)$$

The comparison between extrapolated and correlated friction factor is shown in Figure 15. The correlation field within the error band ±15 %. is shown in Figure 16, where the absolute average deviation between extrapolated and correlated data is 8.7 %.

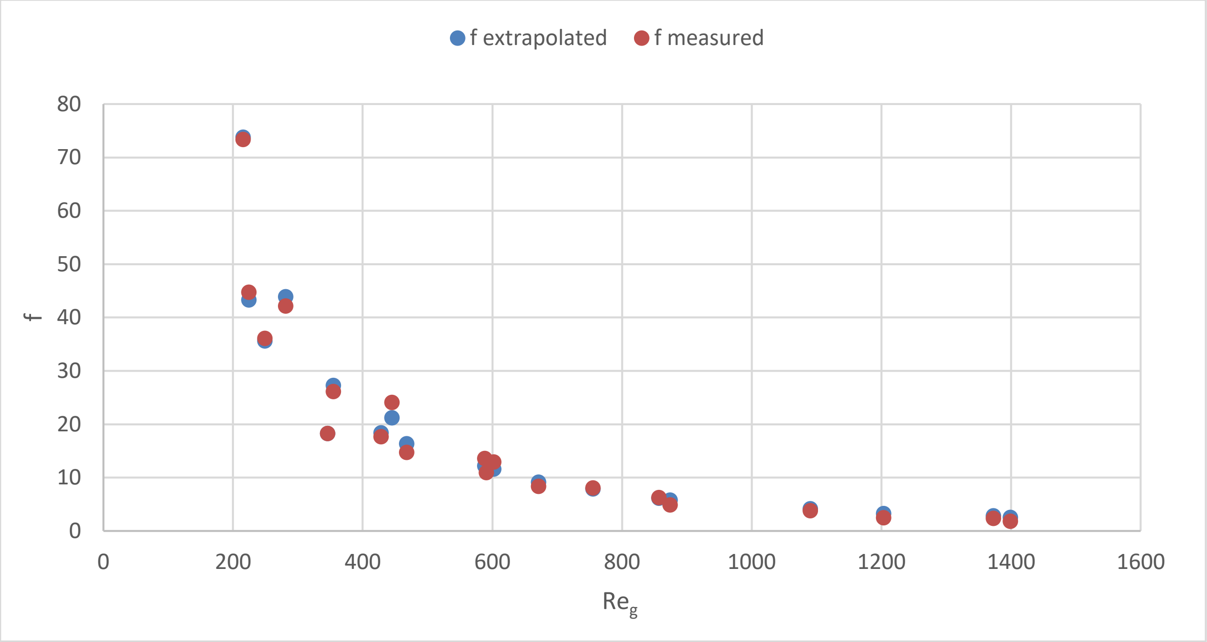

**Figure 15: Fanning friction factor as a function of vapor phase Reynolds number.**

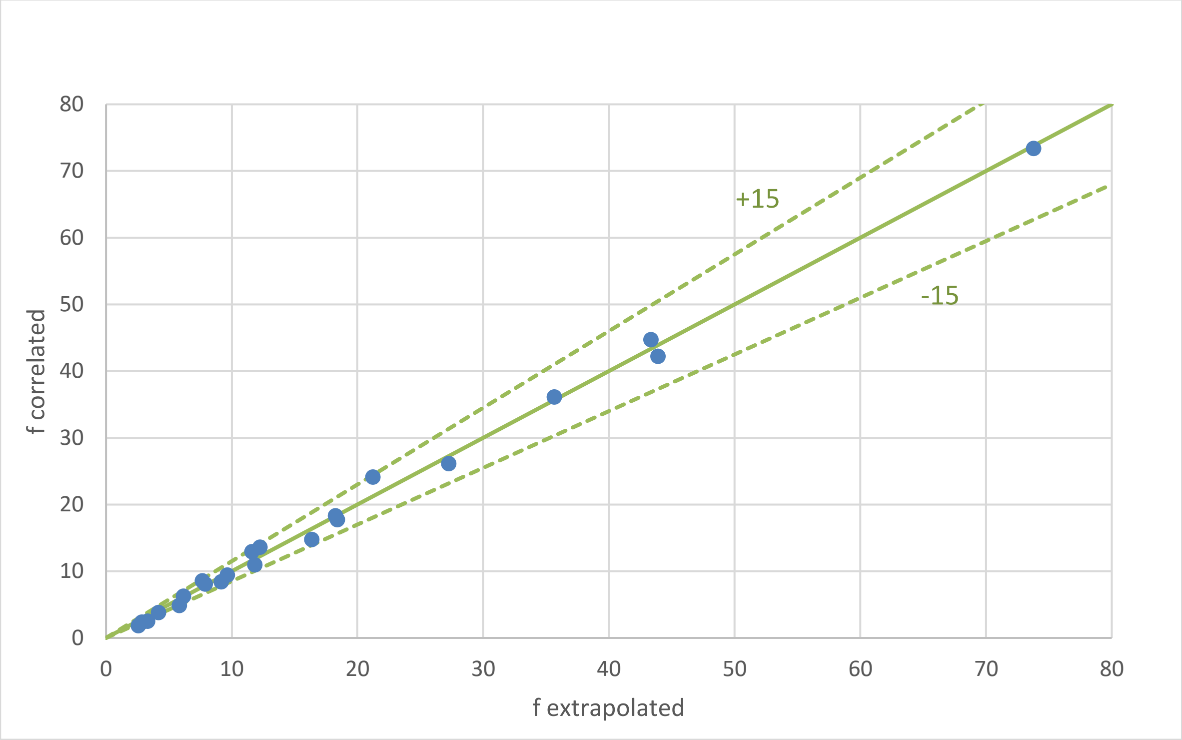

**Figure 16: Correlation field between extrapolated and correlated fanning friction factors.**

### 4.3.2 Heat transfer correlation

As it was previously discussed, the heat transfer coefficient is significantly affected by the presence of the non-condensable gases in the water/steam mixture and its concentration. As well as the rate of the wall temperature undercooling caused by the coolant medium. Heat transfer coefficient value also changed locally that is not possible to capture by the available instrumentation. To estimate the average heat transfer coefficient from the measured data, following process is used:

The overall heat resistance for steady state can be expressed as:

$$\frac{1}{UA} = \frac{LMTD}{Q} = R_{overall} = R_{steam} + R_{wall} + R_{CO2} = \frac{1}{(\eta_0\ htc\ A)_{steam}} + \frac{t}{(kA)_{wall}} + \frac{1}{(\eta_0\ htc\ A)_{CO2}} \quad (4\text{-}7)$$

Then the heat resistance on the steam side can be rewritten as:

$$R_{steam} = \frac{LMTD}{Q} - \frac{t}{(kA)_{wall}} - \frac{1}{(\eta_0\ htc\ A)_{CO2}} = \frac{1}{(\eta_0\ htc\ A)_{steam}} \quad (4\text{-}8)$$

Then the heat transfer coefficient on the sCO$_2$ side can be estimated using the Gnielinsky correlation [14], it goes as:

$$htc = \frac{(\xi/8)RePr}{1 + 12.7\sqrt{(\xi/8)}(Pr^{2/3} - 1)} \cdot \left[1 + \left(\frac{D_h}{L}\right)^{2/3}\right]\left(\frac{k}{D_h}\right) \quad (4\text{-}9)$$

Where $\xi$ goes as:

$$\xi = (1.8log_{10}Re - 1.5)^{-2} \quad (4\text{-}10)$$

Since the heat exchanger concept contains fins, the total heat transfer rate is evaluated through a concept of total surface effectiveness $\eta_0$ defined as:

$$\eta_0 = 1 - (1 - \eta_f)\frac{A_f}{A} \qquad (4\text{-}11)$$

Where $A_f$ is the fin surface area and $A$ is the total surface area, the $\eta_f$ is the fin efficiency defined as:

$$\eta_f = \frac{\tanh(h'X)}{h'X} \qquad (4\text{-}12)$$

Where X is defined as:

$$X = \sqrt{\frac{2\ htc}{k_s\ t}} \qquad (4\text{-}13)$$

The value of $h'$ term for the $CO_2$ channel, which is sandwiched between the steam channels, where the adiabatic plane can be considered in the middle of the channel, thus $h' = h/2 - t$.

The fin surface area $A_f$ is considered as:

$$A_f = 2(H - t) \cdot L \cdot N \qquad (4\text{-}14)$$

Where $N$ is number of channels and $L$ is their effective length. The total area is considered as:

$$A = 2(P - t) \cdot L \cdot N + A_f \qquad (4\text{-}15)$$

Finally, the heat transfer coefficient can be expressed as:

$$htc = \frac{1}{R_{steam}\ (\eta_0\ A)_{steam}} \qquad (4\text{-}16)$$

Where the final value is reached after a couple of iterations due to the changing total surface effectiveness term, where the first iteration is based on the initial guess of the *htc*. The extrapolated averaged htc values on the steam side for each case are present in Figure 17.

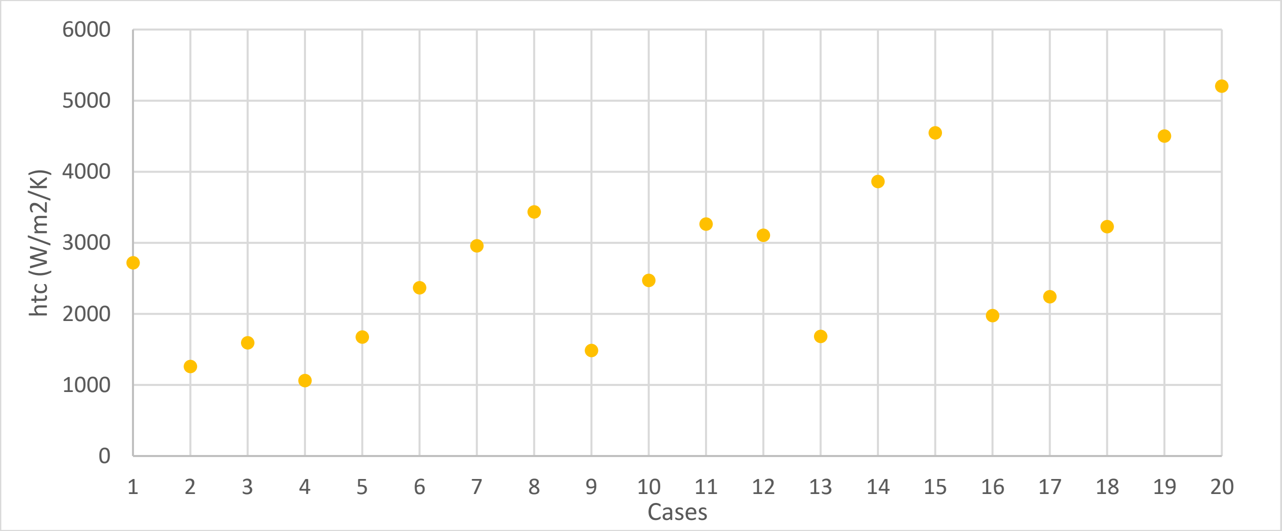

**Figure 17: Extrapolated values of heat transfer coefficients on the steam side.**

Now the Nusselt number on the steam/water side can be calculated as [15]:

$$Nu = \frac{htc}{k_l}\left(\frac{\mu_l^2}{\rho_l(\rho_l-\rho_g)g}\right)^{1/3} \tag{4-17}$$

To account for the effects of the non-condensable gases and the cooling rate, while predicting the average Nusselt number, a following expression was proposed:

$$Nu = C\ Re_l^m\ Pr_l^n\ W_g^o\left(\frac{G_{coolant}}{G_{stean}}\right)^p \tag{4-18}$$

Where *C*, *m*, *n*, *o*, *p* are constants, $Re_l$ is the Reynolds number of the liquid phase, defined as:

$$Re_l = \frac{G\ D_h}{\mu_l} \tag{4-19}$$

The thermophysical properties were obtained from the database NIST [16]. Using the least square linear regression method, following constants were found to match the calculated average Nusselt number:

$$Nu = 1.22\cdot 10^{-5}\ Re_l^{1.49}\ Pr_l^{0.61}\ W_g^{0.85}\left(\frac{G_{coolant}}{G_{stean}}\right)^{0.97} \tag{4-20}$$

The comparison between extrapolated and correlated average Nusselt number is shown in Figure 18. The correlation field within the error band ±30 %. is shown in Figure 19, where the absolute average deviation between extrapolated and correlated data is 10.2 %.

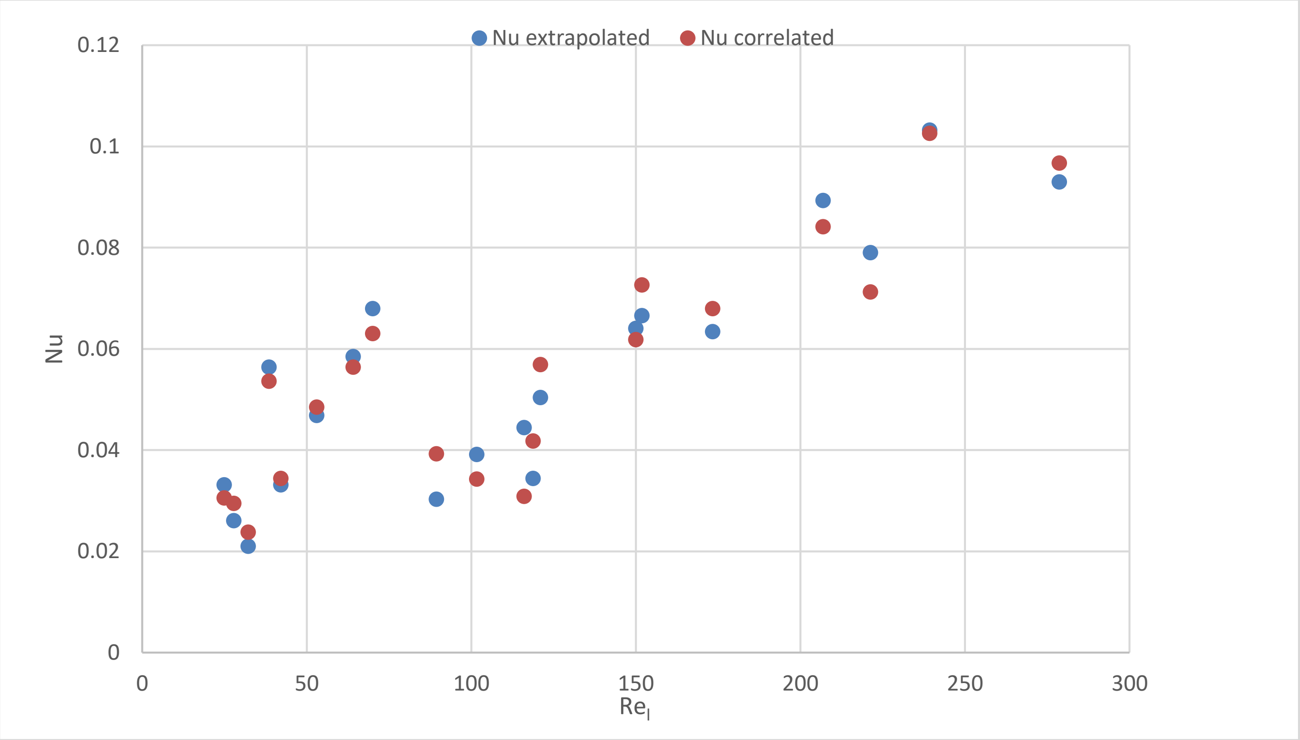

**Figure 18: Comparison of extrapolated and correlated values of average Nusselt numbers on the steam side as a function of Reynolds number.**

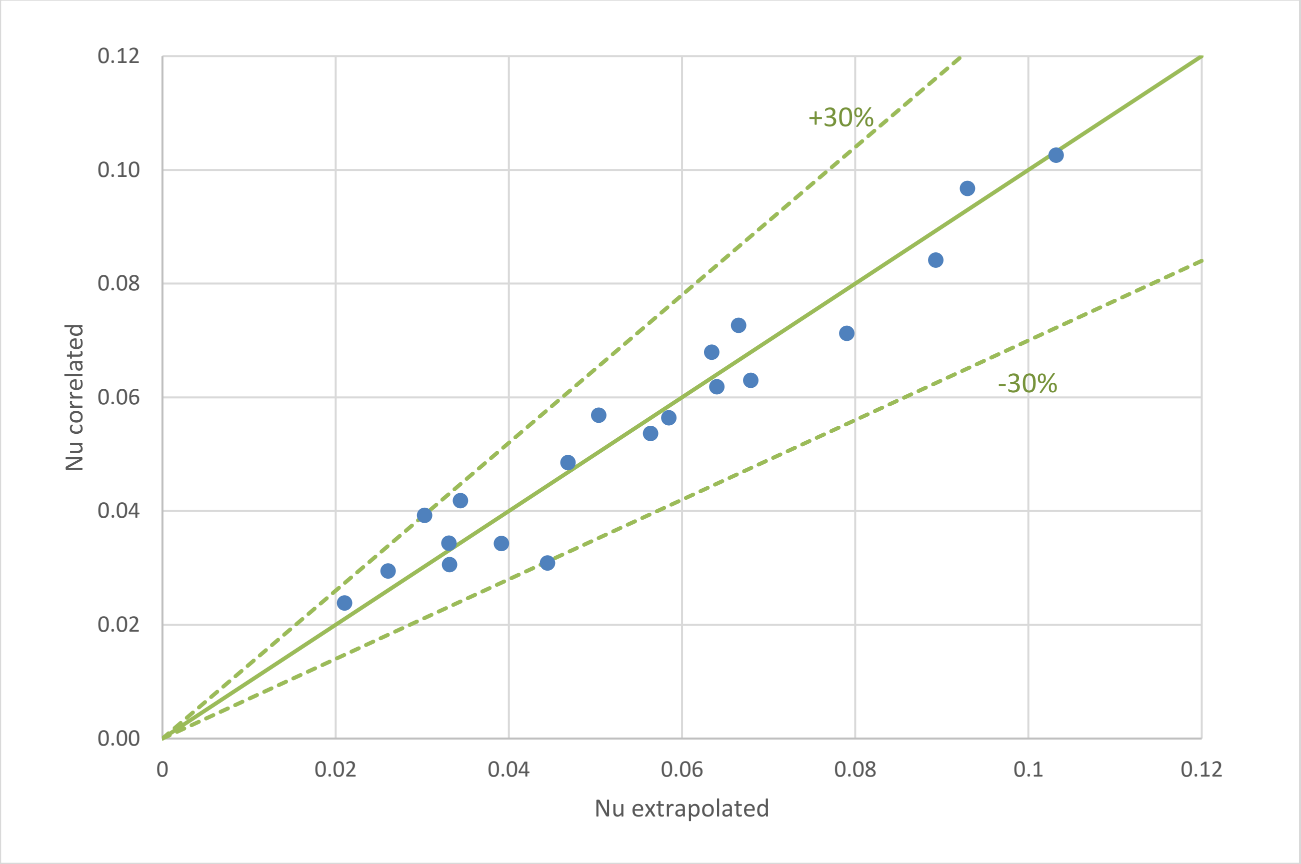

**Figure 19: Correlation field between extrapolated and correlated Nusselt numbers.**

# 5 Mechanical design strategy and final design of the heat recovery exchanger

## 5.1 Final heat exchanger thermal, hydraulic and mechanical design and the estimated performances

The CHX steam produced inside steam generator condense due to $sCO_2$ flow. The CHX is designed for a specified heat transferred of 10 MW. The design idea (Figure 20) is a patent pending technology since it allows heat exchange in a highly compact volume.

Fives Cryo achieved this goal by a double mechanical design strategy:

- ➔ First, this patented configuration allows to bind the latent heat of the steam before confronting it to the cold $sCO_2$, allowing this way to control and optimally reduce the thermal gradients between fluids to ensure the mechanical integrity and high resistance of the heat exchanger component,

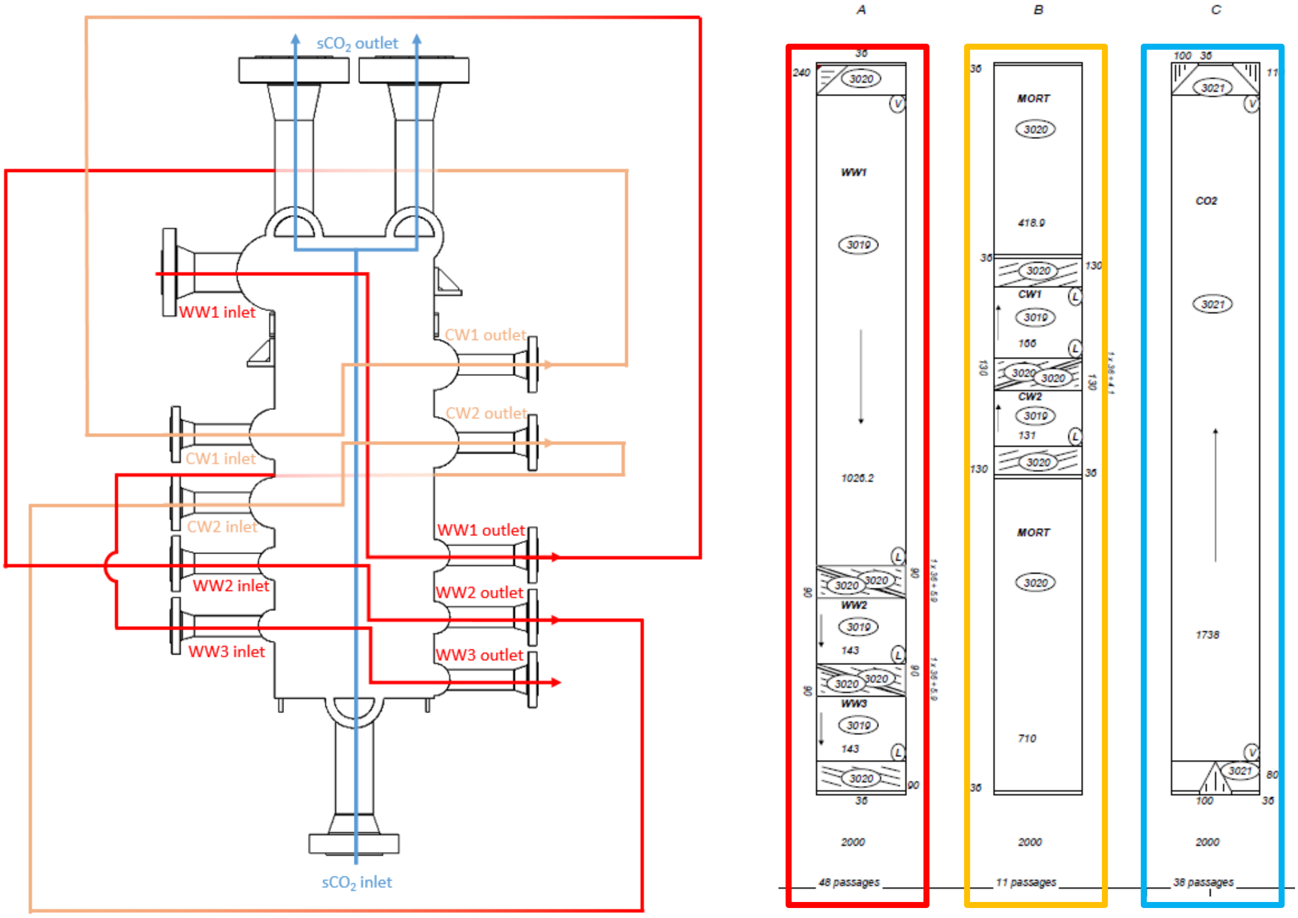

**Figure 20: Schematic drawing of the fluids circulation inside the CHX. The water/steam fluid is decomposed into several sub-fluids WW for Warm Water and CW for Cold Water ©Fives Cryo.**

- ➔ And second, an important work was achieved on material selection according to the data available in the literature. The first results, presenting a variety of metallic alloys specifically used for very high temperature and pressure applications, needed to be crossed with the brazing procedure recommendations and the specific nuclear regulations, which tightened very quickly the field of possibilities. The optimal choice for our application here is the Nickel based alloy N06690 / NC30Fe / Inconel 690. All the specifications related to this material and the appropriate filler metal for welding are reported in Deliverable 4.7. Nevertheless, before reaching the final step of manufacturing such an equipment with this alloy, since Fives Cryo has no previous experience with brazing procedure of this specific material, tests and lab experiments need to be achieved to ensure the adequacy of the brazed joints with the requirements of the nuclear regulations. As explained in Deliverable 4.7, brazing is still an assembly technique under assessment for acceptance by the nuclear regulations.

The CHX design was achieved to lead specifically to one very compact heat exchanger.

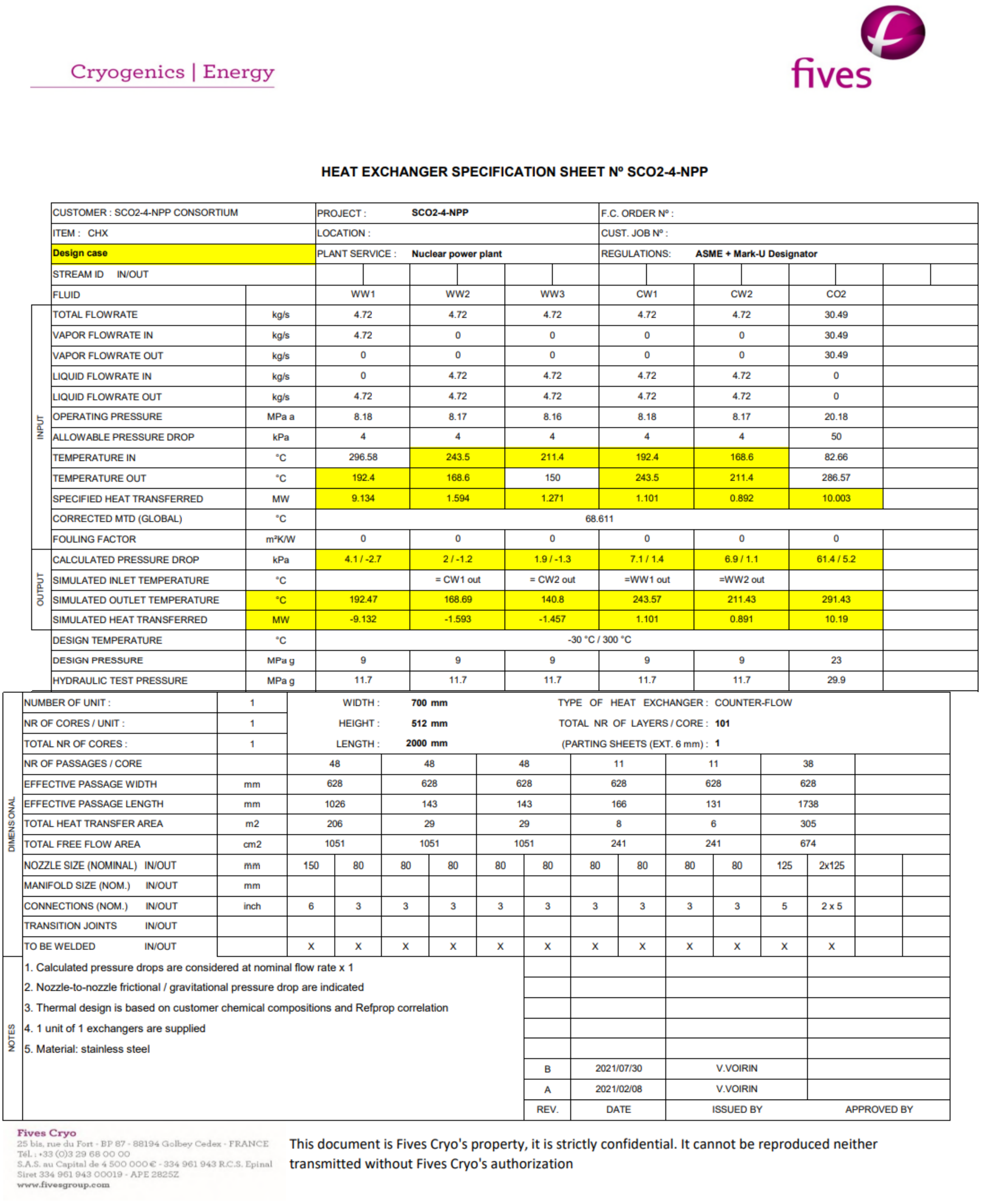

Cryogenics | Energy

**HEAT EXCHANGER SPECIFICATION SHEET Nº SCO2-4-NPP**

CUSTOMER : SCO2-4-NPP CONSORTIUM
ITEM : CHX
**Design case**
PROJECT : **SCO2-4-NPP**
LOCATION :
PLANT SERVICE : **Nuclear power plant**
F.C. ORDER Nº :
CUST. JOB Nº :
REGULATIONS: **ASME + Mark-U Designator**

| | | | | | | | | | |
|---|---|---|---|---|---|---|---|---|---|
| | STREAM ID IN/OUT | | | | | | | | |
| | FLUID | | WW1 | WW2 | WW3 | CW1 | CW2 | CO2 | |
| INPUT | TOTAL FLOWRATE | kg/s | 4.72 | 4.72 | 4.72 | 4.72 | 4.72 | 30.49 | |
| | VAPOR FLOWRATE IN | kg/s | 4.72 | 0 | 0 | 0 | 0 | 30.49 | |
| | VAPOR FLOWRATE OUT | kg/s | 0 | 0 | 0 | 0 | 0 | 30.49 | |
| | LIQUID FLOWRATE IN | kg/s | 0 | 4.72 | 4.72 | 4.72 | 4.72 | 0 | |
| | LIQUID FLOWRATE OUT | kg/s | 4.72 | 4.72 | 4.72 | 4.72 | 4.72 | 0 | |
| | OPERATING PRESSURE | MPa a | 8.18 | 8.17 | 8.16 | 8.18 | 8.17 | 20.18 | |
| | ALLOWABLE PRESSURE DROP | kPa | 4 | 4 | 4 | 4 | 4 | 50 | |
| | TEMPERATURE IN | °C | 296.58 | 243.5 | 211.4 | 192.4 | 168.6 | 82.66 | |
| | TEMPERATURE OUT | °C | 192.4 | 168.6 | 150 | 243.5 | 211.4 | 286.57 | |
| | SPECIFIED HEAT TRANSFERRED | MW | 9.134 | 1.594 | 1.271 | 1.101 | 0.892 | 10.003 | |
| | CORRECTED MTD (GLOBAL) | °C | 68.611 | | | | | | |
| | FOULING FACTOR | m²K/W | 0 | 0 | 0 | 0 | 0 | 0 | |
| OUTPUT | CALCULATED PRESSURE DROP | kPa | 4.1 / -2.7 | 2 / -1.2 | 1.9 / -1.3 | 7.1 / 1.4 | 6.9 / 1.1 | 61.4 / 5.2 | |
| | SIMULATED INLET TEMPERATURE | °C | | = CW1 out | = CW2 out | =WW1 out | =WW2 out | | |
| | SIMULATED OUTLET TEMPERATURE | °C | 192.47 | 168.69 | 140.8 | 243.57 | 211.43 | 291.43 | |
| | SIMULATED HEAT TRANSFERRED | MW | -9.132 | -1.593 | -1.457 | 1.101 | 0.891 | 10.19 | |
| | DESIGN TEMPERATURE | °C | -30 °C / 300 °C | | | | | | |
| | DESIGN PRESSURE | MPa g | 9 | 9 | 9 | 9 | 9 | 23 | |
| | HYDRAULIC TEST PRESSURE | MPa g | 11.7 | 11.7 | 11.7 | 11.7 | 11.7 | 29.9 | |

DIMENSIONAL

| | | |
|---|---|---|
| NUMBER OF UNIT : | 1 | WIDTH : **700 mm** |
| NR OF CORES / UNIT : | 1 | HEIGHT : **512 mm** |
| TOTAL NR OF CORES : | 1 | LENGTH : **2000 mm** |

TYPE OF HEAT EXCHANGER : COUNTER-FLOW
TOTAL NR OF LAYERS / CORE : **101**
(PARTING SHEETS (EXT. 6 mm) : **1**

| | | | | | | | | |
|---|---|---|---|---|---|---|---|---|
| NR OF PASSAGES / CORE | | 48 | 48 | 48 | 11 | 11 | 38 | |
| EFFECTIVE PASSAGE WIDTH | mm | 628 | 628 | 628 | 628 | 628 | 628 | |
| EFFECTIVE PASSAGE LENGTH | mm | 1026 | 143 | 143 | 166 | 131 | 1738 | |
| TOTAL HEAT TRANSFER AREA | m2 | 206 | 29 | 29 | 8 | 6 | 305 | |
| TOTAL FREE FLOW AREA | cm2 | 1051 | 1051 | 1051 | 241 | 241 | 674 | |

| | | | | | | | | | | | | | | |
|---|---|---|---|---|---|---|---|---|---|---|---|---|---|---|
| NOZZLE SIZE (NOMINAL) IN/OUT | mm | 150 | 80 | 80 | 80 | 80 | 80 | 80 | 80 | 80 | 80 | 125 | 2x125 | | |
| MANIFOLD SIZE (NOM.) IN/OUT | mm | | | | | | | | | | | | | | |
| CONNECTIONS (NOM.) IN/OUT | inch | 6 | 3 | 3 | 3 | 3 | 3 | 3 | 3 | 3 | 3 | 5 | 2 x 5 | | |
| TRANSITION JOINTS IN/OUT | | | | | | | | | | | | | | | |
| TO BE WELDED IN/OUT | | X | X | X | X | X | X | X | X | X | X | X | X | | |

NOTES

1. Calculated pressure drops are considered at nominal flow rate x 1
2. Nozzle-to-nozzle frictional / gravitational pressure drop are indicated
3. Thermal design is based on customer chemical compositions and Refprop correlation
4. 1 unit of 1 exchangers are supplied
5. Material: stainless steel

| | | | |
|---|---|---|---|
| B | 2021/07/30 | V.VOIRIN | |
| A | 2021/02/08 | V.VOIRIN | |
| REV. | DATE | ISSUED BY | APPROVED BY |

**Fives Cryo**
25 bis, rue du Fort - BP 87 - 88194 Golbey Cedex - FRANCE
Tél. : +33 (0)3 29 68 00 00
S.A.S. au Capital de 4 500 000 € - 334 961 943 R.C.S. Epinal
Siret 334 961 943 00019 - APE 2825Z
www.fivesgroup.com

This document is Fives Cryo's property, it is strictly confidential. It cannot be reproduced neither transmitted without Fives Cryo's authorization

**Figure 21: CHX design datasheet ©Fives Cryo**

The design achieved by Fives led to a single core, which specifications are detailed in Figure 21 with the following dimensions:

- Width: 700 mm
- Height: 512 mm

- Length: 2000 mm

It is a counter-flow heat exchanger with a total number of layers of 101. The layers are distributed as follows:

- 38 layers for $CO_2$
- 59 layers for steam
- 4 “dummy” layers, which are inactive layers, 2 on bottom stacking and 2 on top, to guarantee the mechanical integrity of the heat exchanger cores.

Each layer has a height of 4 mm. Both $CO_2$ and steam/water layers contain “plain” fins but with different geometries, as shown in deliverable D4.4.

The parting sheets between CHX core layers are 1 mm thick, external sheets are 4 mm thick.

This CHX design allows developing a total heat transfer area of 305 $m^2$ for $CO_2$ and of 278 $m^2$ for water steam.

In order to draw a performance map, a maximal operation case was also tested on this design to ensure the capability of the CHX to operate under harsh conditions. The results are detailed in Figure 22.

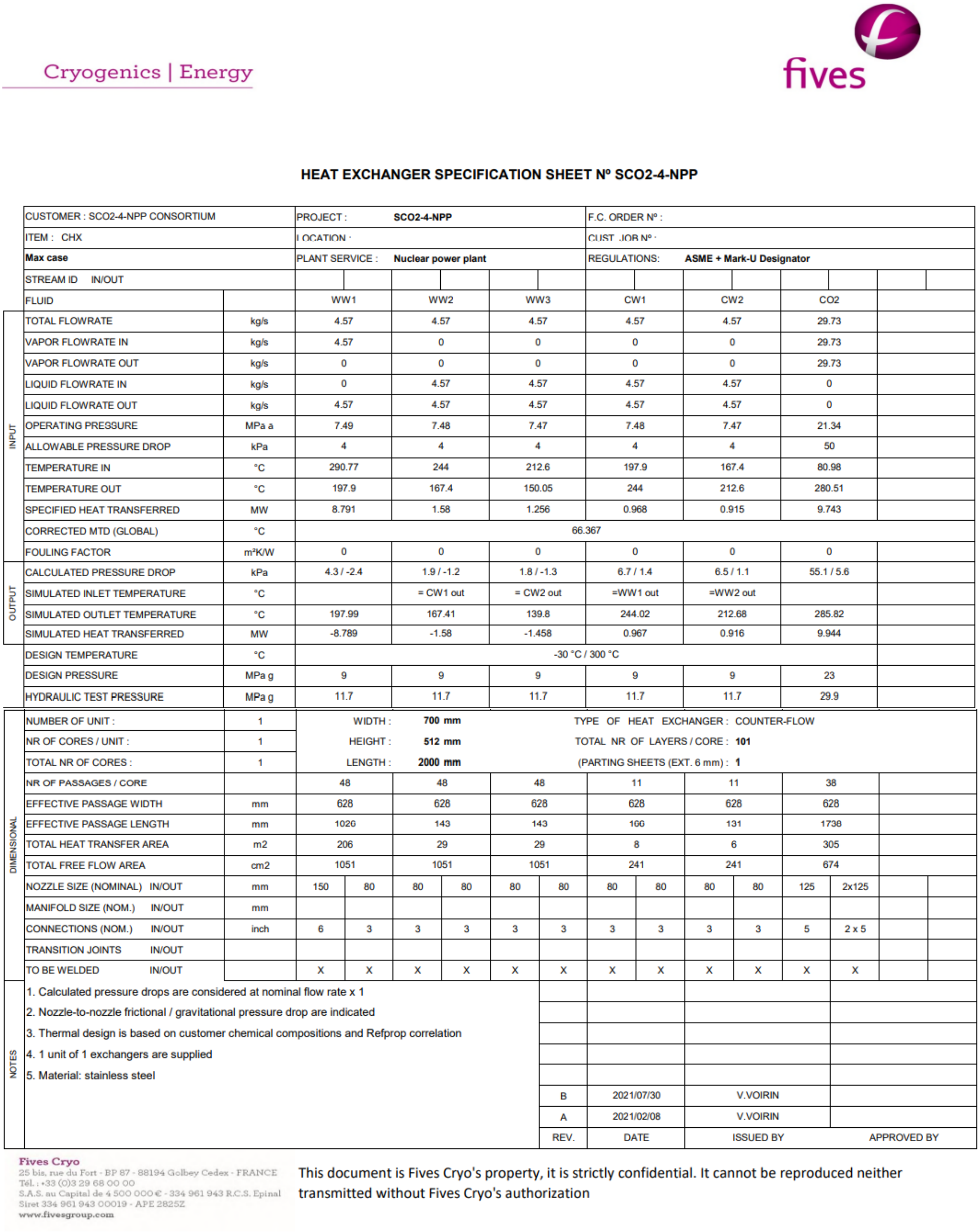

Cryogenics | Energy

fives

**HEAT EXCHANGER SPECIFICATION SHEET Nº SCO2-4-NPP**

| | | |
|---|---|---|
| CUSTOMER : SCO2-4-NPP CONSORTIUM | PROJECT : **SCO2-4-NPP** | F.C. ORDER Nº : |
| ITEM : CHX | LOCATION : | CUST. JOB Nº : |
| **Max case** | PLANT SERVICE : **Nuclear power plant** | REGULATIONS: **ASME + Mark-U Designator** |

| | | | | | | | | | |
|---|---|---|---|---|---|---|---|---|---|
| | STREAM ID IN/OUT | | | | | | | | |
| | FLUID | | WW1 | WW2 | WW3 | CW1 | CW2 | CO2 | |
| INPUT | TOTAL FLOWRATE | kg/s | 4.57 | 4.57 | 4.57 | 4.57 | 4.57 | 29.73 | |
| | VAPOR FLOWRATE IN | kg/s | 4.57 | 0 | 0 | 0 | 0 | 29.73 | |
| | VAPOR FLOWRATE OUT | kg/s | 0 | 0 | 0 | 0 | 0 | 29.73 | |
| | LIQUID FLOWRATE IN | kg/s | 0 | 4.57 | 4.57 | 4.57 | 4.57 | 0 | |
| | LIQUID FLOWRATE OUT | kg/s | 4.57 | 4.57 | 4.57 | 4.57 | 4.57 | 0 | |
| | OPERATING PRESSURE | MPa a | 7.49 | 7.48 | 7.47 | 7.48 | 7.47 | 21.34 | |
| | ALLOWABLE PRESSURE DROP | kPa | 4 | 4 | 4 | 4 | 4 | 50 | |
| | TEMPERATURE IN | °C | 290.77 | 244 | 212.6 | 197.9 | 167.4 | 80.98 | |
| | TEMPERATURE OUT | °C | 197.9 | 167.4 | 150.05 | 244 | 212.6 | 280.51 | |
| | SPECIFIED HEAT TRANSFERRED | MW | 8.791 | 1.58 | 1.256 | 0.968 | 0.915 | 9.743 | |
| | CORRECTED MTD (GLOBAL) | °C | 66.367 | | | | | | |
| | FOULING FACTOR | m²K/W | 0 | 0 | 0 | 0 | 0 | 0 | |
| OUTPUT | CALCULATED PRESSURE DROP | kPa | 4.3 / -2.4 | 1.9 / -1.2 | 1.8 / -1.3 | 6.7 / 1.4 | 6.5 / 1.1 | 55.1 / 5.6 | |
| | SIMULATED INLET TEMPERATURE | °C | | = CW1 out | = CW2 out | =WW1 out | =WW2 out | | |
| | SIMULATED OUTLET TEMPERATURE | °C | 197.99 | 167.41 | 139.8 | 244.02 | 212.68 | 285.82 | |
| | SIMULATED HEAT TRANSFERRED | MW | -8.789 | -1.58 | -1.458 | 0.967 | 0.916 | 9.944 | |
| | DESIGN TEMPERATURE | °C | -30 °C / 300 °C | | | | | | |
| | DESIGN PRESSURE | MPa g | 9 | 9 | 9 | 9 | 9 | 23 | |
| | HYDRAULIC TEST PRESSURE | MPa g | 11.7 | 11.7 | 11.7 | 11.7 | 11.7 | 29.9 | |

| | | | | |
|---|---|---|---|---|
| DIMENSIONAL | NUMBER OF UNIT : | 1 | WIDTH : **700 mm** | TYPE OF HEAT EXCHANGER : COUNTER-FLOW |
| | NR OF CORES / UNIT : | 1 | HEIGHT : **512 mm** | TOTAL NR OF LAYERS / CORE : **101** |
| | TOTAL NR OF CORES : | 1 | LENGTH : **2000 mm** | (PARTING SHEETS (EXT. 6 mm) : **1** |

| | | | | | | | | | |
|---|---|---|---|---|---|---|---|---|---|
| | NR OF PASSAGES / CORE | | 48 | 48 | 48 | 11 | 11 | 38 | |
| | EFFECTIVE PASSAGE WIDTH | mm | 628 | 628 | 628 | 628 | 628 | 628 | |
| | EFFECTIVE PASSAGE LENGTH | mm | 1026 | 143 | 143 | 166 | 131 | 1738 | |
| | TOTAL HEAT TRANSFER AREA | m2 | 206 | 29 | 29 | 8 | 6 | 305 | |
| | TOTAL FREE FLOW AREA | cm2 | 1051 | 1051 | 1051 | 241 | 241 | 674 | |

| | | | | | | | | | | | | | | | |
|---|---|---|---|---|---|---|---|---|---|---|---|---|---|---|---|
| NOZZLE SIZE (NOMINAL) IN/OUT | mm | 150 | 80 | 80 | 80 | 80 | 80 | 80 | 80 | 80 | 80 | 125 | 2x125 | | |
| MANIFOLD SIZE (NOM.) IN/OUT | mm | | | | | | | | | | | | | | |
| CONNECTIONS (NOM.) IN/OUT | inch | 6 | 3 | 3 | 3 | 3 | 3 | 3 | 3 | 3 | 3 | 5 | 2 x 5 | | |
| TRANSITION JOINTS IN/OUT | | | | | | | | | | | | | | | |
| TO BE WELDED IN/OUT | | X | X | X | X | X | X | X | X | X | X | X | X | | |

NOTES

1. Calculated pressure drops are considered at nominal flow rate x 1
2. Nozzle-to-nozzle frictional / gravitational pressure drop are indicated
3. Thermal design is based on customer chemical compositions and Refprop correlation
4. 1 unit of 1 exchangers are supplied
5. Material: stainless steel

| REV. | DATE | ISSUED BY | APPROVED BY |
|---|---|---|---|
| | | | |
| | | | |
| | | | |
| | | | |
| | | | |
| B | 2021/07/30 | V.VOIRIN | |
| A | 2021/02/08 | V.VOIRIN | |

**Fives Cryo**
25 bis, rue du Fort - BP 87 - 88194 Golbey Cedex - FRANCE
Tél. : +33 (0)3 29 68 00 00
S.A.S. au Capital de 4 500 000 € - 334 961 943 R.C.S. Epinal
Siret 334 961 943 00019 - APE 2825Z
www.fivesgroup.com

This document is Fives Cryo's property, it is strictly confidential. It cannot be reproduced neither transmitted without Fives Cryo's authorization

Figure 22: CHX maximal operating case design datasheet ©Fives Cryo

## 5.2 Drawings

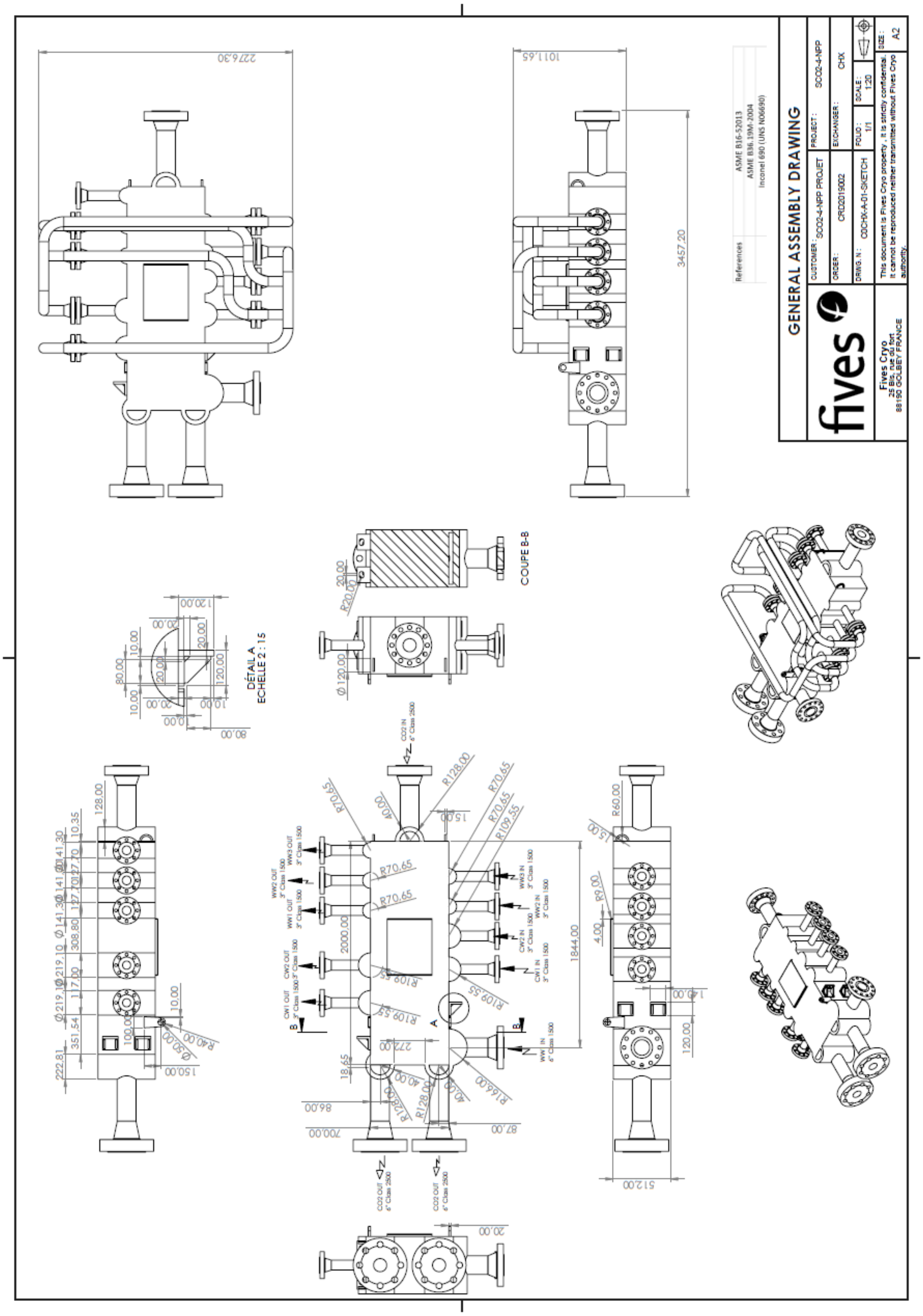

**Figure 23: General assembly drawing of the CHX ©Fives Cryo**

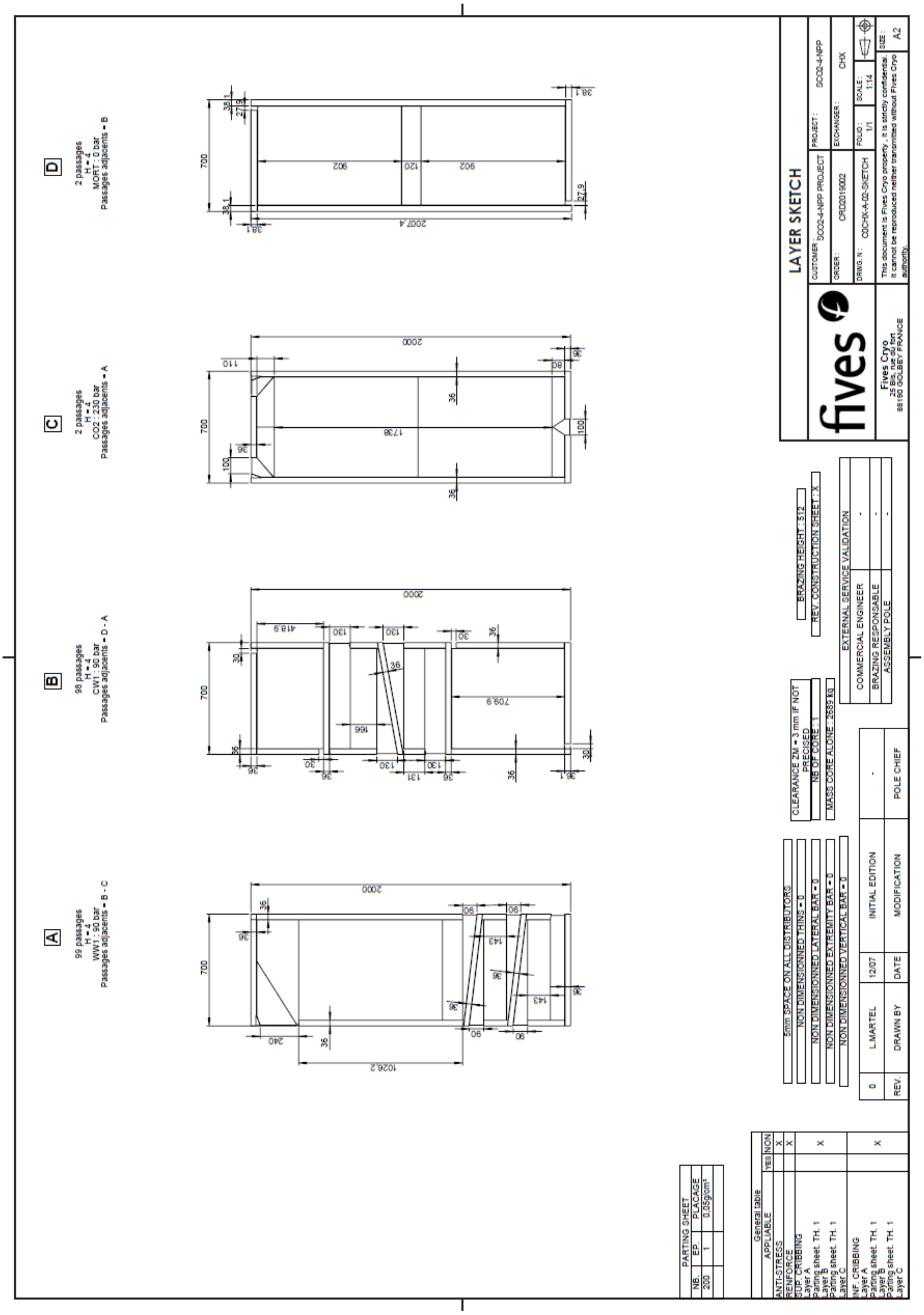

**Figure 24: CHX layers detailed sketch ©Fives Cryo**

## 5.3 Costs

According to the drawings in section 5.2, the CHX component is composed of 1 core with the following dimensions: L 2000 mm x l 700 mm x H 512 mm, for a core matrix volume of 0.72 m$^3$.

The corresponding costs, including the headers equipment, are detailed in Table 3.

**Table 3: CHX costs details**

| | | |
|---|---|---|
| TOTAL Costs of Material | € | 237947 |
| **Manufacturing workforce** | | |
| Fins manufacturing | € | 3000 |
| Parts preparation & stacking | € | 27 000 |
| Brazing alloy application | € | 13 500 |
| Headers welding | € | 81541 |
| TOTAL Manufacturing Workforce | | 125041 |
| **Subcontracting** | | |
| Sheets cutting | € | 8500 |
| Other parts cutting | € | 4000 |
| Brazing in vacuum furnace | €/unit | 4825 |
| TOTAL Subcontracting | | 17325 |
| **External purchase** | | |
| Compression device | € | 4000 |
| TOTAL External purchase | € | 4000 |
| TRANSPORT | € | 1000 |
| **Design office / QC NPP regulation** | | |
| Design office | € | 37120 |
| Internal examination | € | 17000 |
| External examination | € | 2500 |
| TOTAL Design office / QC | € | 56620 |
| **TOTAL CHX costs** | **€** | **695000** |

Fives Cryo is still not equipped with the adequate stamping machine to be able to produce fins out of such very resistant material as Inconel 690. The costs of stamping machine purchasing and adaptation of Fives Cryo's Workshop are also to be taken into account in case of manufacturing of a very low number of heat exchangers. This aspect will be strongly dependent on the market opportunities that the studies achieved during this project may open with the deployment of the sCO$_2$ safety cooling cycle.

Also, the raw material costs (bars, sheets for the fins production, cap sheets and separation sheets, headers and nozzles, etc.) increased exponentially after the Covid crisis, and are still rising. Apart from the manufacturing part, the material cost will be subject to an update at the moment of manufacturing the equipment. Hopefully, when it is time, the economic crisis will remain behind us.

# 6 Conclusion

The steam condensation in the tiny channels during the natural circulation was experimentally tested on the representative heat exchanger mockup, based on the preliminary design of the CHX, at different flow regimes corresponding with the real operating conditions. The experimental data also accounts for the presence of the non-condensable gases, whose effect was already discussed in section 3. This effect as well as the correction for the ratio of the flow coolant/condensate was considered and the heat transfer correlation was proposed. The proposed heat transfer correlation fits the measured data with an average absolute deviation of 10.2 %. Furthermore, the fanning friction factor during the condensation was extrapolated and put into the correlation. The proposed correlation fits the measured data with an average absolute deviation of 8.7 %. The gathered data can help to verify the numerical codes regarding the thermal-hydraulic design of the condensers.

Fives Cryo compiled the available data and proposed the mechanical design strategy and the final design of the CHX unit, based on their in house software. The corresponding drawings and the estimated costs are included. However, there are still some challenges, such as brazing the suitable alloys to withstand the operational pressures (22 MPa on the $sCO_2$ side), as well as meeting the requirements for the nuclear standards.

Finally, it is recommended to consider adding the possibility to degas continually or periodically the non-condensable gases from the multiple inlet/outlet tubing on the CHX unit, since there is a high possibility for them to accumulate and prevent the proper functioning of the heat exchanger.

# 7 References

[1] “sCO2-4-NPP.” https://www.sco2-4-npp.eu/ (accessed Aug. 09, 2022).

[2] J. Venker, “Development and validation of models for simulation of supercritical carbon dioxide Brayton cycles and application to self-propelling heat removal systems in boiling water reactors,” 2015.

[3] M. Strätz, R. Mertz, and J. Starflinger, “Experimental investigation on the heat transfer between condensing steam and sCO2 in a compact heat exchangers,” in *2nd European sCO2 Conference*, Aug. 2018, pp. 135–144. doi: 10.17185/duepublico/46078.

[4] K. Theologou, M. Hofer, R. Mertz, M. Buck, E. Laurien, and J. Starflinger, “Experimental investigation and modelling of steam-heated supercritical CO2 compact cross-flow heat exchangers,” *Appl Therm Eng*, vol. 190, p. 116352, May 2021, doi: 10.1016/J.APPLTHERMALENG.2020.116352.

[5] Straetz and M. Ralf, “2018-sCO2 . eu-104 EXPERIMENTAL INVESTIGATION ON THE HEAT TRANSFER BETWEEN CONDENSING STEAM AND SCO 2 IN A COMPACT HEAT EXCHANGER,” 2018.

[6] S. Tioual-Demange and V. Voirin, “Deliverable D4.4 Preliminary design and models of the sCO2-4-NPP heat exchangers.” https://www.sco2-4-npp.eu/ (accessed Aug. 09, 2022).

[7] P. J. Marto, “Condensation,” in *Handbook of Heat transfer*, 3rd ed., W. M. Rohsenow, J. P. Hartnett, and C. I. Young, Eds. 1998, pp. 926–988.

[8] S. T. Revankar and D. Pollock, “Laminar film condensation in a vertical tube in the presence of noncondensable gas,” *Appl Math Model*, vol. 29, no. 4, pp. 341–359, Apr. 2005, doi: 10.1016/J.APM.2004.09.010.

[9] V. F. Tyapkov and S. F. Erpyleva, “Water chemistry of the secondary circuit at a nuclear power station with a VVER power reactor,” *Thermal Engineering*, vol. 64, no. 5, pp. 357–363, May 2017, doi: 10.1134/S0040601517050081.

[10] P. Kral, J. Hyvarinen, A. Prosek, and A. Guba, “SOURCES AND EFFECT OF NON-CONDENSABLE GASES IN REACTOR COOLANT SYSTEM OF LWR,” Aug. 2015.

[11] V. Voirin, “FC-FS-CHX mockup-revA.” https://projectsworkspace.eu/sites/sCO2-4-NPP/CollaborativeDocuments/FC-FS-CHX%20mockup-revA.pdf (accessed Aug. 11, 2022).

[12] A. Vojáček, “SCO2 EXPERIMENTAL LOOP AND CVR R&D ACTIVITIES,” Sep. 01, 2017. http://www.sco2-hero.eu/wp-content/uploads/2017/09/03_Vojacek_CVR_sCO2-experimental-loop-and-CVR-RD-activities.pdf (accessed Aug. 09, 2022).

[13] M. Doan, T. Dang, and X. Nguyen, “The Effects of Gravity on the Pressure Drop and Heat Transfer Characteristics of Steam in Microchannels: An Experimental Study,” *Energies (Basel)*, vol. 13, no. 14, 2020, doi: 10.3390/en13143575.

[14] V. Gnielinski, “Heat Transfer in Pipe Flow,” in *Heat Atlas VDI*, 2010, pp. 693–699.

[15] P. J. Marto, “Condensation,” in *Handbook of Heat transfer*, 3rd ed., W. M. Rohsenow, J. P. Hartnett, and C. I. Young, Eds. 1998, pp. 926–988.

[16] E. W. Lemmon, and Ian H. Bell, M. L. Huber, and M. O. McLinden, “NIST Standard Reference Database 23: Reference Fluid Thermodynamic and Transport Properties-REFPROP, Version 10.0, National Institute of Standards and Technology.” 2018. doi: https://doi.org/10.18434/T4/1502528.